

République Algérienne Démocratique et Populaire

Ministère de l'Enseignement Supérieure et de la Recherche Scientifique

Université Abderrahmane Mira- Béjaïa



Faculté de la Technologie

Département d'Automatique, Télécommunication et d'Electronique

Projet de Fin d'Etudes

Pour l'obtention du diplôme de Master en

Filière : ELECTRONIQUE

Spécialité : INSTRUMENTATION

Thème

Étude comparative des techniques de maximisation de puissance d'un module photovoltaïque

Préparé par :

BERKAINE Ghiles

SAMKANGE Tinotenda Ronald

Dirigé par :

M. HANFOUG

Examiné par :

M. SADJI P

Mme. OUALI E

Année universitaire: 2022/202

People's Democratic Republic of Algeria

Ministry of Higher Education and Scientific Research

University of Abderrahmane Mira- Béjaïa



Faculty of Technology

Department of Automation, Telecommunication and Electronics

Project

For obtaining the Master's degree in

Field: ELECTRONICS

Speciality: INSTRUMENTATION

Theme

**Comparative study of power maximization techniques
of a photovoltaic module**

Prepared by:

BERKAINE Ghiles

SAMKANGE Tinotenda Ronald

Directed by:

M. HANFOUG

Examined by:

M. SADJI P

Mme. OUALI E

Academic year: 2022/2023

Acknowledgements

WE ARE GRATEFUL, ABOVE ALL, TO THE ALMIGHTY FOR BESTOWING UPON US THE WILLPOWER TO SEE THIS ENDEAVOR THROUGH, WHICH STANDS AS THE RESULT OF SEVERAL YEARS OF STUDY.

THIS THESIS WOULD NOT HAVE COME TO FRUITION WITHOUT THE PRECIOUS COLLABORATION OF MANY INDIVIDUALS WHOM WE WISH TO THANK.

WE WOULD LIKE TO EXTEND OUR DEEPEST GRATITUDE AND ACKNOWLEDGMENT TO OUR SUPERVISOR, MR. HANFOUG, FOR GRACIOUSLY AGREEING TO MENTOR THIS PROJECT, AS WELL AS FOR HIS UNWAVERING SCIENTIFIC AND MORAL SUPPORT.

LASTLY, WE WOULD LIKE TO EXPRESS OUR APPRECIATION TO THE ESTEEMED JURY MEMBERS WHO HAVE HONORED US BY EVALUATING THIS HUMBLE WORK. **THANK YOU ALL.**

Dedication

I HUMBLY DEDICATE THIS HUMBLE WORK TO MY MOTHER, WHO PATIENTLY WAITED FOR THE FRUITS OF HER GOOD UPBRINGING AND AFFECTION. TO MY FATHER, WHO SHOWED ME THE RIGHT PATH AND REMINDED ME THAT WILLPOWER ALWAYS SHAPES GREAT INDIVIDUALS.

AND TO MY DEAR FRIENDS, EACH NAMED INDIVIDUALLY, YOUR FRIENDSHIP HAS BROUGHT LIGHT AND JOY TO MY LIFE. I AM ETERNALLY GRATEFUL FOR YOUR GENUINE FRIENDSHIP AND UNWAVERING SUPPORT THROUGHOUT THIS JOURNEY. THANK YOU FROM THE BOTTOM OF MY HEART.

BERKAINÉ Ghiles

THIS STUDY IS WHOLEHEARTEDLY DEDICATED TO MY FAMILY AND FRIENDS TO WHOM I AM GREATLY INDEBTED FOR THEIR UNWAVERING SUPPORT.

TO MY PARENTS, I HOPE THAT THIS ACHIEVEMENT JUSTIFIES AND SHOWS MY GRATITUDE TO ALL THE SACRIFICES YOU'VE MADE THROUGHOUT MY ACADEMIC JOURNEY.

SAMKANGE Tinotenda Ronald

Table of Contents

Acknowledgements	I
Dedication	II
Table of contents	III
List of table	IV
List of figures	VII
Symbols and abbreviation	XI
General Introduction	1
Chapter I Solar cells	3
I.1 Introduction	3
I.2 The solar energy	3
I.2.1 The sun.....	4
I.2.2 The solar spectrum.....	4
I.3 The semi-conductors	5
I.3.1 The Energy bands	5
I.3.2 The doping	6
I.3.3 The PN junction	7
I.4 The solar cell	7
I.4.1 The Principle of operation of a solar cell.....	8
I.4.2 The structure of solar cell	9
I.4.3 The electrical characteristics.....	10
I.4.4 The equivalent circuit of a solar cell.....	10
I.5 The Photovoltaic module.....	11
I.5.1 The cells in series association.....	12
I.5.2 The cells in parallel association	12
I.5.3 The Photovoltaic effect.....	13
I.5.4 The Photovoltaic conversion	14
I.6 The characteristics of solar cells.....	15
I.6.1 The short-circuit current density	15
I.6.2 The open circuit voltage	15
I.6.3 The fill factor	16
I.6.4 The conversion efficiency.....	16

I.7	The types of photovoltaic cells	16
I.8	Conclusion	18
Chapter II MPPT Techniques and DC-DC converters		19
II.1	Introduction	19
II.2	The MPPT Solar Charge Controller	19
II.2.1	The DC-DC Converter.....	20
II.2.2	The Boost Converter	21
II.3	The Maximum Power Point (MPP)	25
II.4	The various algorithms used for MPPT.....	25
II.4.1	Perturb and Observe (P&O).....	25
II.4.1.1	Principle	25
II.4.1.2	Algorithm.....	26
II.4.1.3	Advantages and disadvantages of P&O	28
II.4.2	Particle swam optimization PSO	29
II.4.2.1	Principle	29
II.4.2.2	Algorithm.....	30
II.4.2.3	Advantages and disadvantages of PSO.....	31
II.4.3	Incremental Conductance	32
II.4.3.1	Principle	32
II.4.3.2	Algorithm.....	32
II.4.3.3	Advantages and disadvantages of IC	33
II.5	Conclusion	34
Chapter III Simulation and Results		35
III.1	Introduction	35
III.2	The Simulation of the photovoltaic system.....	35
III.2.1	Simulation of the BOOST converter	35
III.2.2	Simulations of the module without MPPT	37
III.2.3	Simulations with MPPT for each method at STC	38
III.2.4	Perturb and Observe method.....	40
III.2.5	Incremental Conductance Method	46
III.2.6	Particle swam optimization method.....	49
III.3	Comparison between the 3 MPPT methods (P&O, INC, PSO).....	53
III.3.1	Response and tracking speed	53
III.3.2	Accuracy and oscillations at MPP	54

III.3.3	Settling time	54
III.3.4	Stability under changing conditions	55
III.3.5	Table of comparisons.....	57
III.4	Conclusion.....	58
General Conclusion	60
Bibliography	62
Abstract	67
Résumé	68

List of Tables

Chapter I**Table I-1:** The different types of cells with their efficiency.....18**Chapter II****Table II-1:** Summary of Perturb and observe algorithm.....27**Table II-2:** Summary of Incremental Conductance algorithm.....32**Chapter III****Table III-1:** Value of components.....36**Table III-2:** Settling time.....55**Table III-3:** Summary of comparisons between P&O, IC and PSO.....57

List of Figures

Chapter I The Solar cells

Figure I-1: Global incident solar energy, expressed in kWh/m ² per year.....	3
Figure I-2: Wavelength of the AM 0 and AM 1.5G spectra.....	4
Figure I-3: Categorization of materials according to the energy band theory.....	6
Figure I-4: Doping of silicon.....	7
Figure I-5: Formation of a PN junction.....	7
Figure I-6: Basic structure of solar cell	8
Figure I-7: Operating principle of a photovoltaic cell	9
Figure I-8: I-V characteristic of a solar cell in the dark and under illumination.....	10
Figure I-9: The equivalent electrical circuit of a photovoltaic cell.....	11
Figure I-10: Components of a photovoltaic panel field	11
Figure I-11: Diagram of PV cells associated in series	12
Figure I-12: I-V characteristics of cells connected in series	12
Figure I-13: Diagram of PV cells connected in parallel	13
Figure I-14: I-V characteristics of cells connected in parallel	13
Figure I-15: Schematic presentation of a solar cell	14
Figure I-16: Current voltage (IV) cure of a solar cell.....	16
Figure I-17: Pictures depicting various kinds of photovoltaic cells.....	17

Chapter II The MPPT Techniques and DC-DC converters

Figure II-1: MPPT charge controller.....	19
Figure II-2: Diagram of an MPPT controlled solar panel.....	20
Figure II-3: DC-DC converter in PV system.....	21
Figure II-4: Circuit diagram of a Boost converter.....	21
Figure II-5: Boost converter with switch ON and diode OFF.....	22
Figure II-6: Boost converter when switch is OFF and diode is ON.....	23
Figure II-7: Voltage waveforms of V_{pv} and V_{load} when considering a Boost converter.....	24
Figure II-8: MPP on I-V and P-V curves.....	25
Figure II-9: Operating characteristic of P&O method.....	27
Figure II-10: Algorithm for P&O.....	28
Figure II-11: PSO flowchart.....	31
Figure II-12: Operating characteristic of Incremental Conductance method.....	33

Figure II-13: Algorithm for Incremental Conductance.....	33
Chapter III Simulation and Results	
Figure III-1: Boost converter circuit.....	35
Figure III-2: Graph comparing V_{in} and V_{out} of Boost converter.....	37
Figure III-3: PV module parameters.....	37
Figure III-4: I-V and P-V characteristic curve of the module.....	38
Figure III-5: PV current at $\Delta\alpha = 0.001$ and $\Delta\alpha = 0.01$	38
Figure III-6: PV voltage at $\Delta\alpha = 0.001$ and $\Delta\alpha = 0.01$	39
Figure III-7: PV power at $\Delta\alpha = 0.001$ and $\Delta\alpha = 0.01$	39
Figure III-8: Simulink diagram of a PV system using the P&O method.....	40
Figure III-9: PV current using the P&O method.....	40
Figure III-10: PV voltage using the P&O method.....	41
Figure III-11: Load voltage (across resistor) using the P&O method.....	41
Figure III-12: PV power using the P&O method.....	41
Figure III-13: Variation of irradiance with time.....	42
Figure III-14: Variation on I_{pv} under changing irradiance conditions.....	42
Figure III-15: Variation on V_{pv} under changing irradiance conditions.....	43
Figure III-16: Variation on P_{pv} under changing irradiance conditions.....	43
Figure III-17: Variation of temperature with time.....	44
Figure III-18: Variation on I_{pv} under changing temperature conditions.....	44
Figure III-19: Variation on V_{pv} under changing temperature conditions.....	45
Figure III-20: Variation on P_{pv} under changing temperature conditions.....	45
Figure III-21: Simulink diagram of a PV system with IC technique.....	46
Figure III-22: PV current using the IC method.....	46
Figure III-23: PV voltage using the IC method.....	46
Figure III-24: Load voltage (across resistor) using the IC method.....	47
Figure III-25: PV power using the IC method.....	47
Figure III-26: Variation of irradiance with time.....	48
Figure III-27: Variation on P_{pv} under changing irradiance conditions.....	48
Figure III-28: Variation of temperature with time.....	48
Figure III-29: Variation on P_{pv} under changing temperature conditions.....	49
Figure III-30: Simulink diagram of a PV system using the PSO method.....	49
Figure III-31: PSO parameters	49
Figure III-32: PV current using PSO.....	50

Figure III-33: PV voltage using PSO.....	50
Figure III-34: Load voltage (across resistor) using PSO.....	50
Figure III-35: PV power using PSO.....	51
Figure III-36: Variation of irradiance with time.....	51
Figure III-37: Variation on Ppv under changing irradiance conditions.....	52
Figure III-38: Variation of temperature with time.....	52
Figure III-39: Variation on Ppv under changing temperature conditions	52
Figure III-40: Comparing PV power of P&O, IC, PSO.....	53
Figure III-41: Comparing oscillations of Ppv at MPP.....	54
Figure III-42: Comparing oscillations of Vload at MPP.....	54
Figure III-43: Rapidly varying irradiance.....	55
Figure III-44: PV power under rapidly varying irradiance.....	56
Figure III-45: Slowly varying irradiance.....	56
Figure III-46: PV power under slowly varying irradiance	57

Symbols

λ	the wavelength
c_1 and c_2	Acceleration constants
I_{ph}	Photocurrent
s_t^k	Particle position in the search space at iteration k
G_{best}	Global best
P_{best}	Local best
V_{ref}	Reference voltage
c	Speed of light
D	Duty cycle
eV	Electron Volt
h	Planck's constant.
I	Current
I_{mpp}	Current at MPP
I_{sc}	Short circuit current
K	Boltzmann constant ($K = 1.38 \times 10^{-23} J.K^{-1}$)
N	Population size
P	Power
q	Charge of the electron ($q = 1.6 \times 10^{-19} c$)
T	Temperature
V	Voltage
v	Particle velocity
V_{mpp}	Voltage at MPP
V_{oc}	Open Circuit Voltage
V_{soc}	Open Circuit Voltage (series association)
w	Inertia weight factor
W_p	Peak Watts
ΔP	Change in power
$\Delta \alpha$	Duty cycle step size
η	Conversion efficiency
n	The ideality factor of the diode

Abbreviations

AC	Alternating current
AM	Air Mass
AM 1.5G	Air Mass 1.5 Global
AM0	Air Mass Zero
DC	Direct current
FF	Fill Factor
IC	Incremental Conductance
MPP	Maximum Power Point
MPPT	Maximum Power Point Tracking
P&O	Perturb and Observe
PSO	Particle Swarm Optimization
PV	Photovoltaic
PWM	Pulse Width Modulation

General

Introduction

General Introduction

Recently, solar energy is proving to be one of the alternative solutions to our dependence on fossil fuels. This clean, inexhaustible energy can provide ten thousand times more energy than that consumed by the entire world population. As a result, developing this sector remains a priority for many countries in order to achieve sustainable development on these three dimensions: economic, social and environmental [1]

Photovoltaic (PV) cells offer the possibility of directly generating electricity from solar radiation, without the need for moving parts, heat production, or causing atmospheric, local, or global pollution. Technological advancements have been significant since the early photovoltaic cells, which, due to their high cost and low efficiency, were primarily intended for highly specific applications such as powering satellites.

The use of the power maximization techniques such as MPPT systems is essential in photovoltaic energy conversion systems. These enable PV systems to extract the maximum power output from the solar panel, which varies based on factors such as solar radiation and temperature. The MPPT technique controls the duty cycle of the DC-DC converter, ensuring optimal system performance across different operating conditions. [2]

This project focused on studying various MPPT techniques and their implementation in maximizing the power output of PV modules. The primary objective was to evaluate the performance of different MPPT techniques in terms of energy efficiency and stability. The research outcomes will contribute to enhancing the overall efficiency of solar systems and promoting more efficient utilization of solar energy as a renewable power source.

This master's thesis is divided into three (3) chapters.

- **The first chapter** explores the fundamental concepts of solar cell technology. It begins by examining the characteristics of the sun and its electromagnetic spectrum, highlighting the diverse range of radiation that can be utilized by PV cells. The subsequent section of the chapter centers around semiconductors and their role in solar cells. It covers topics such as energy bands, doping, and PN junctions. Furthermore, it emphasizes the photovoltaic components and the photovoltaic effect, which facilitate the conversion of light energy into electrical energy. The chapter then delves into various types of solar cells, their functionalities, structures, characteristics, and equivalent circuits.
- **In the second chapter**, we will explore the application of MPPT techniques, specifically Perturb & Observe, Incremental Conductance, and Particle Swarm Optimization, in optimizing the energy production of photovoltaic systems. These

techniques are designed to maximize power output by dynamically adjusting the duty cycle of DC-DC converters thus extracting maximum power from PV modules.

- **The third chapter** focuses on the practical implementation of MPPT techniques using MATLAB's SIMULINK tool. It presents a prescribed photovoltaic system and simulates the performance of different MPPT algorithms, including Perturb & Observe, Particle Swarm Optimization, and Incremental Conductance. The simulation evaluates the effectiveness of each technique in tracking the maximum power point (MPP) of the PV module under varying environmental conditions. The results provide valuable insights into the design and selection of an appropriate MPPT algorithm for specific PV systems.

We conclude this dissertation with a general conclusion, some perspectives and future prospects.

The Solar Cells

I.1 Introduction

Solar energy has emerged as a promising source of renewable energy in recent years. The sun, the most abundant source of energy in our solar system, emits a spectrum of radiation that can be harnessed by PV cells to generate electricity. In this chapter, we will explore the different aspects of solar cell technology.

To begin our discussion, we will cover different aspects of solar power such as the sun and the solar spectrum. After that, we will delve into semiconductors and investigate the fundamental ideas of energy bands, doping and the PN junction. These concepts are critical to the operation of solar cells.

Next, we will delve into photovoltaic modules, where we will discuss photovoltaic conversion and the photovoltaic effect, which allow solar cells to convert light energy into electrical energy.

Finally, we will focus on solar cells themselves, discussing their principle of operation, structure, characteristics, and equivalent circuit, and exploring the different types of solar cells that are available.

I.2 The solar energy

The source of solar energy is the result of nuclear fusion reactions that take place at the core of the Sun, it is essentially an enormous fusion reactor. [3] Its waste is recycled and it is confined by robust magnetic fields. It is, without a doubt, the primary source of energy for the Earth. Interestingly, coal, oil, and natural gas are also products of the Sun's activity. These fossil fuels are the result of the prolonged decomposition and transformation of organic matter, such as plants, that originally utilized solar energy for growth through photosynthesis. [4]

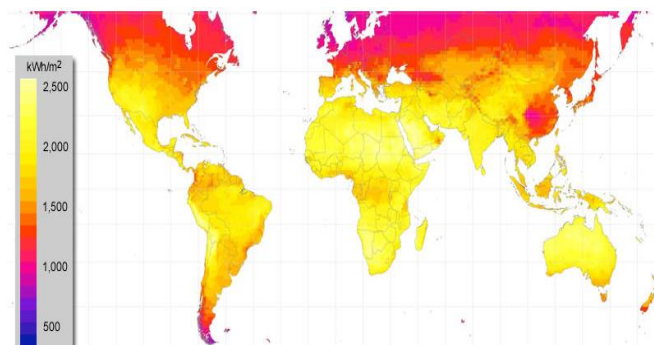


Figure I-1: Global incident solar energy, expressed in kWh/m² per year.

I.2.1 The sun

The star that is nearest to our planet is the sun, and it is situated at a distance of 150 million kilometers. The Sun is an enormous sphere of gas that consists primarily of 70% hydrogen and 28% helium, with the remaining 2% being comprised of the majority of other atoms found throughout the universe. Over 60 different chemical elements have been discovered on the sun. By fusing hydrogen and helium atoms together, the sun is able to achieve temperatures as high as 20 million degrees Kelvin.

The sun supplies an enormous amount of energy to the earth's surface, equivalent to 6,000 times the world's current energy consumption, with an estimated output of 120,000 TW. Despite this, capturing solar energy and converting it into useful forms such as electricity, heat, or chemical fuels using inexpensive and readily available materials is still a significant challenge. Photovoltaic cells are expected to play a vital role in finding environmentally sustainable solutions to this energy issue. [5] [6] [7]

I.2.2 The solar spectrum

The release of energy leads to the production of radiation that is primarily composed of wavelengths within the 0.2 μ m to 3 μ m range. When beyond the atmosphere, the sun's emitted radiation (AM0) is comprised of:

- 9% Ultraviolet ($0.1 < \lambda < 0.4\mu\text{m}$)
- 43% visible ($0.4 < \lambda < 0.75\mu\text{m}$)
- 48% infrared ($0.75 < \lambda < 5\mu\text{m}$)

A spectrum is used to illustrate the radiation and its intensity with respect to the wavelength of the AM 0 and AM 1.5G spectra. (**Figure I-2**)

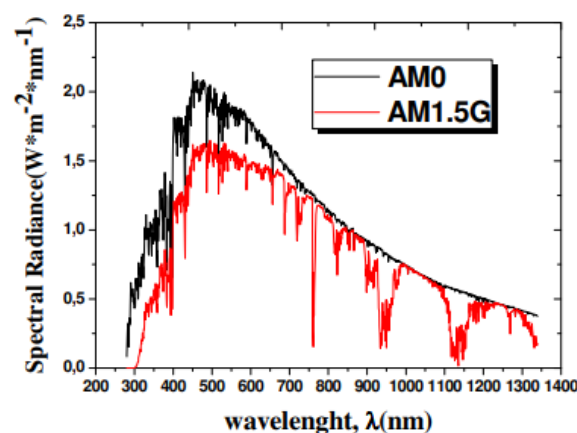


Figure I-2: the wavelength of the AM 0G and AM 1.5G spectra. [8]

One can observe that the atmosphere causes significant absorption at specific wavelengths.

The solar spectrum consists of electromagnetic radiation with wavelengths ranging from 290nm to 2770nm, which includes ultraviolet rays, visible light, and infrared rays. The atmosphere of the Earth functions as a filter that absorbs some of the radiation due to the presence of various gases. Air Mass (AM) is a measure of the amount of power absorbed by the atmosphere based on the position of the sun relative to the zenith. It quantifies the reduction in the power of light as it passes through the atmosphere and is absorbed by air and dust. The AM 0 solar spectrum refers to the solar spectrum outside of the Earth's atmosphere and is mainly utilized in space applications, with a power of roughly 1.36 kW/m². On the other hand, the AM 1.5G spectrum represents the solar spectrum at sea level on Earth during clear weather conditions when the sun is at the zenith at an angle of 48°, with a power of approximately 1 kW/m². [9]

The AM 1.5G spectrum is characterized by the fact that the path of light through the atmosphere is 1.5 times longer than the shortest distance from the sun. The term "G" refers to global radiation.

To qualify photovoltaic modules, the standard conditions require an AM1.5 spectrum exposure at an irradiance of 1000W/m² and a temperature of 25°C.

I.3 The semi-conductors

Semiconductors are substances that have electrical conductivity that lies between that of conductors and insulators. The electrical conductivity of semiconductors is highly influenced by temperature. Such materials possess outermost electrons that are distributed between two energy bands with a relatively narrow energy gap of approximately 1eV. [10]

I.3.1 The Energy bands [11]

➤ Conductor

Conductors like silver, copper, aluminum, gold, iron, steel, etc., have a significant number of free electrons at room temperature, which means that there is no energy gap. As a result, the valence band and the conduction band are overlapping.

➤ Insulator

Insulators such as wood, paper, mica, plastic, etc., have a significant energy gap of around 7 electron volts (7 eV). As a result, even at high temperatures or voltages, electrons

cannot move from the valence band to the conduction band. This property prevents these materials from conducting electricity altogether.

➤ Semiconductor

Semiconductors like Silicon, germanium, etc., behave like an insulator at absolute zero temperature since the conduction band is empty. However, at normal or room temperature, some electrons can move from the valence band to the conduction band, allowing the semiconductor to conduct partially.

As the temperature increases, the energy gap between the valence band and the conduction band decreases, and a greater number of free electrons become available, leading to increased conductivity.

- At normal or room temperature, the energy gap of Silicon and Germanium is 1.12 electron volts (1.12 eV) and 0.78 electron volts (0.78 eV), respectively.
- Semiconductors are materials that have electrical conductivity between that of conductors (metals) and insulators, with a lower conductivity than metals but higher than insulators.

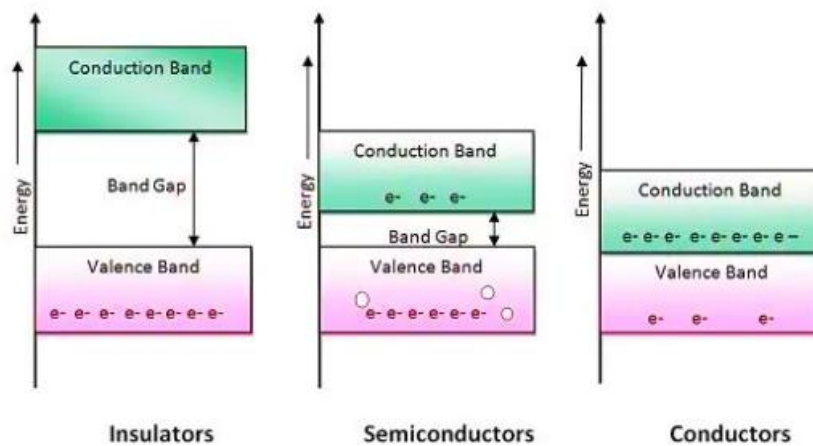


Figure I-3: Categorization of materials according to the energy band theory (where e- stands for electrons and o represents holes). [11]

I.3.2 The doping [10]

The introduction of additional energy levels due to any alteration in the periodicity of the lattice is considered as a defect. However, doping a pure semiconductor, which is known as "intrinsic," can lead to an increase in the number of excess charges, which ultimately results in the improvement of the material's conductivity. (**Figure I-4**).

A substance introduced into a lattice at a substitution position, which has more valence electrons than the atom in the lattice, is known as a donor. Common examples of such elements include those from group V of the periodic table, such as P, As, and Sb. This leads to the semiconductor being classified as N-type.

An acceptor is an impurity that replaces an atom in a lattice, and it has fewer valence electrons than the atom it replaces. Group III atoms (B, Al, GA) in a crystalline lattice made of Si are an example of acceptors. This creates a P-type semiconductor, where the majority carriers are holes.

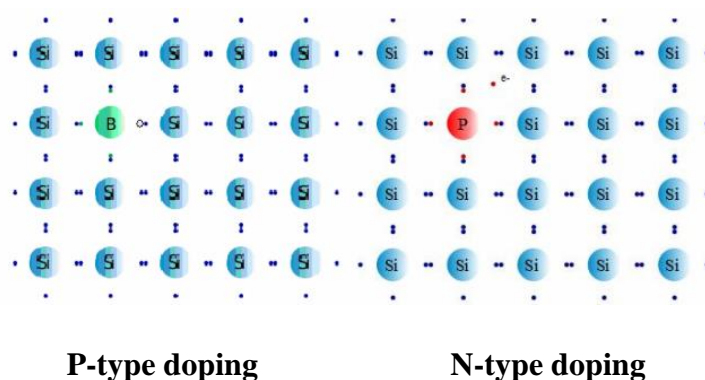


Figure I-4: Doping of silicon.

I.3.3 The PN junction

The process of creating a PN junction involves placing a P-doped semiconductor (known as the anode) next to an N-doped semiconductor (known as the cathode), both made from the same monocrystalline semiconductor material [12]. This is illustrated in (Figure I-5). When these two types of semiconductors come into contact, a transient electrical state is established on either side of the junction, followed by a permanent state. A simple junction forms a diode.

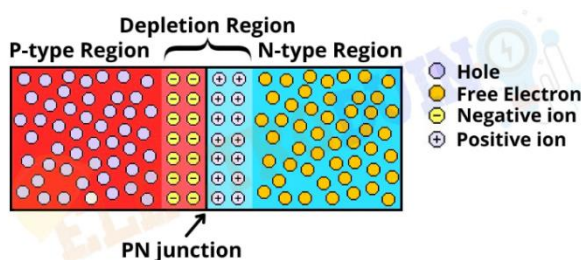


Figure I-5: Formation of a PN junction. [13]

I.4 The solar cell

The main purpose of a photovoltaic cell, which is essentially a specialized photodiode, is to generate a current flow consisting of electrons when it is exposed to light irradiation, by

utilizing the photovoltaic effect. For the best possible outcome, the junction through which light enters the semiconductor must be thin enough to enable most of the light to pass over the active region (known as the depletion region), where it can be transformed into electron/hole pairs [14] [15].

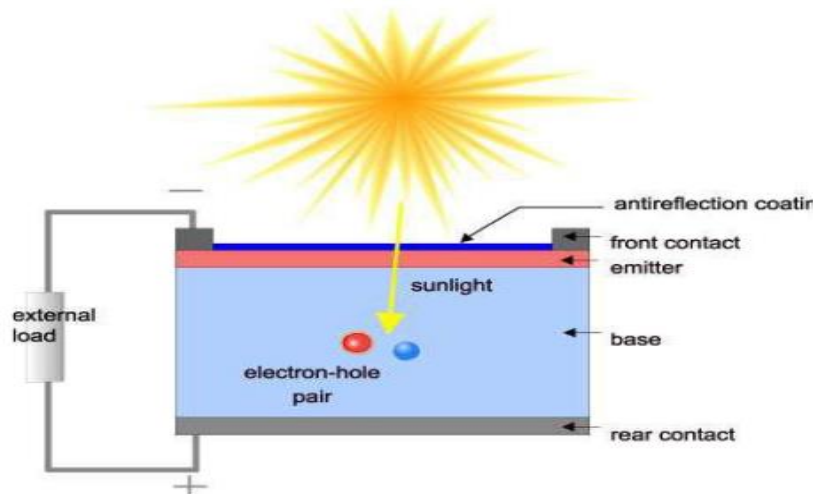


Figure I-6: Basic structure of solar cell.

I.4.1 The Principle of operation of a solar cell

Solar cells use the photovoltaic effect to convert sunlight directly into electricity by creating and transporting positive and negative electric charges in a semiconductor material. This material is made up of two parts, one with extra electrons and the other with fewer electrons, known as type N and type P doped areas. When the N-doped and P-doped areas are connected, excess electrons from the N material move into the P material. As a result, the previously N-doped area becomes positively charged and the previously P-doped area becomes negatively charged, creating an electric field that drives electrons towards the N area and holes towards the P area, forming a PN junction. By attaching metallic contacts to the N and P areas, a diode is created. When the junction is exposed to light, photons with energy greater than the band gap energy promote electrons from the valence band to the conduction band, leaving a hole behind, resulting in the creation of an electron-hole pair. If an external load is connected to the cell, the electrons flow from the N area to the P area through the external connection, generating a potential difference and an electric current. [16]

(**Figure I-7**) depicts how a solar cell functions. When photons strike the cell, they produce carriers in both the N and P regions, as well as the space charge zone. The behavior of these

carriers depends on where they were generated. In regions where there is no electric charge, such as the N and P regions, minority photo-carriers move around through diffusion.

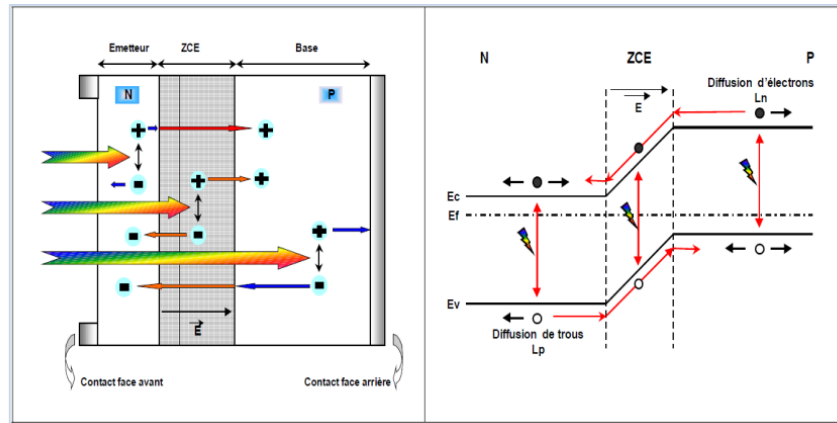


Figure I-7: Operating principle of a photovoltaic cell [17].

The free carriers created by incident photons behave differently depending on their location. Those that end up in the space charge region are pushed by the electric field towards the region where they become the majority carriers. This diffusion of photo-carriers results in a diffusion photocurrent. In the space charge region, the electric field dissociates the electron-hole pairs created by photons, with the electrons moving towards the N-type region and the holes towards the P-type region. This generation of carriers generates a generation photocurrent. The combination of these two contributions results in a photocurrent I_{ph} that contributes to the reverse current of the diode.

I.4.2 The structure of solar cell

The makeup of a solar cell is comparable to a PN junction, and the formula provided gives the dark current in this type of structure. [18]

$$I_{obs} = I_s \left[\exp\left(\frac{qV}{nKT}\right) - 1 \right] \quad (\text{I-1})$$

I_{obs} : The current under darkness.

I_s : The saturation current of the diode.

q : Charge of the electron ($q = 1.6 \times 10^{-19} \text{ C}$);

V : Applied voltage.

K : Boltzmann constant ($K = 1.38 \times 10^{-23} \text{ J.K}^{-1}$);

T : Absolute temperature in Kelvin.

And under illumination, the current is given by the formula:

$$I = I_{obs} - I_{ph} = I_s \left[\exp\left(\frac{qV}{nKT}\right) - 1 \right] - I_{ph} \quad (\text{I-2})$$

With:

I_{ph} : Photocurrent of the diode.

n : Ideality factor of the diode.

I.4.3 The electrical characteristics

The way in which the current "A" (or current density "A/cm²") changes depending on the voltage "V" can be used to assess how well a solar cell is performing, both in the absence of light and especially when exposed to it. Two examples of the characteristics of a solar cell's I-V curve are shown in **(Figure I-8)** - one with illumination and one without [19].

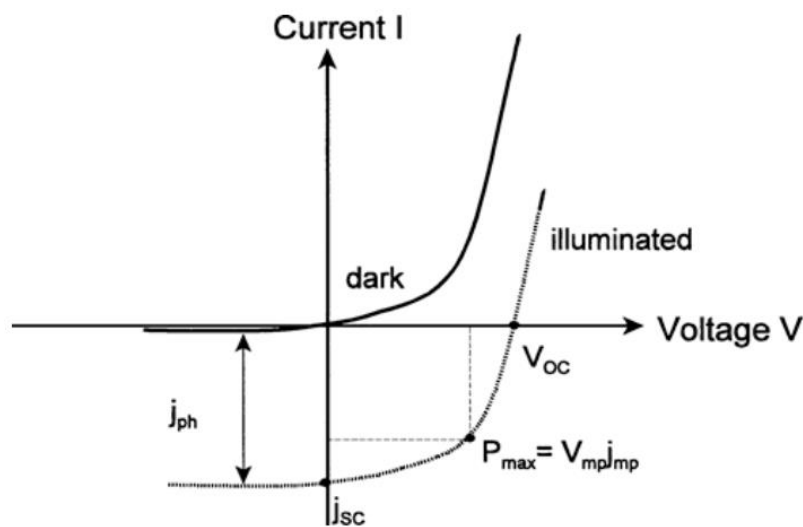


Figure I-8: I-V characteristic of a solar cell in the dark and under illumination. [20]

I.4.4 The equivalent circuit of a solar cell

There are several electric models, also known as equivalent circuits, for reproducing the behavior of a cell using electronic components. The most common circuits are those with one or two diodes. This circuit is presented as follows in **(Figure I-9)**

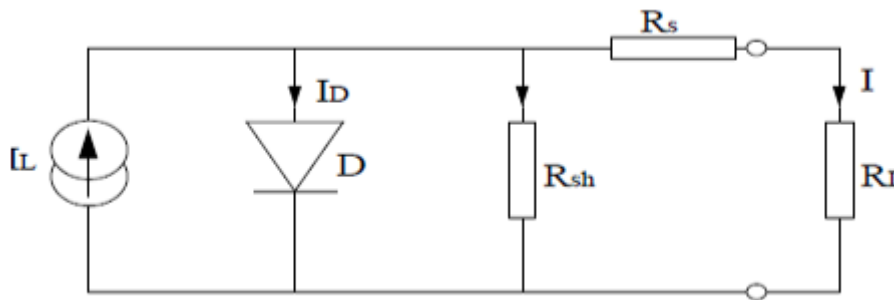


Figure I-9: The equivalent electrical circuit of a photovoltaic (PV) cell [21]

- The current source I_L represents the current I_{ph} generated by the illumination.
- The shunt resistance R_{sh} models the parasitic currents flowing through the cell.
- The series resistance R_s models the ohmic losses of the material. This resistance should be as low as possible to minimize its influence on the solar cell's performance.
- In the ideal case, R_s is equal to zero and R_{sh} tends to infinity.
- The load resistance R_L represents the external circuit's resistance when the cell is connected.
- The diode D is a blocking diode that prevents battery discharge through the PV cell in the absence of sunlight.

I.5 The Photovoltaic module

The definition of a photovoltaic module is a group of solar cells that are put together to generate electricity when exposed to sunlight. Individually, a solar cell only produces a small amount of electricity, typically around 1 to 3 watts with a voltage below 1 volt. Therefore, multiple cells are combined to create a photovoltaic module that can produce more power.

If you connect several cells in a series, the voltage will rise for the same electrical current. Conversely, connecting them in parallel will increase the current while keeping the voltage constant. A set of photovoltaic modules that are placed together on a single surface is known as a panel. The total of all panels in a system is known as a photovoltaic array, as demonstrated in (Figure I-10). [22]

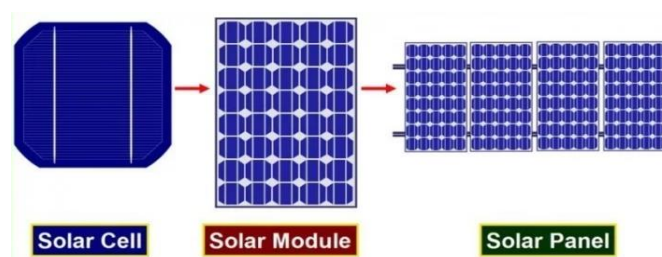


Figure I-10: Components of a photovoltaic panel field. [23]

I.5.1 The cells in series association [24]

When components are connected in series, they experience the same current flow, and their combined characteristic can be determined by adding up the individual voltages and currents. The resulting characteristic can be seen in (**Figure I-12**), which shows the voltage and current (V_{soc} , I_{sc}) of N_s identical cells (V_{oc} , I_{cc}) connected in series. The current in a series grouping is limited by the lowest current among the cells, and therefore during production, all cells are tested and sorted based on their performance.

$$I_{sc}=I_{cc} \text{ And } V_{soc}=N_s \times V_{oc} \quad (\text{I-3})$$

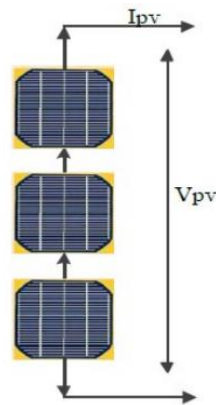


Figure I-11: Diagram of PV cells associated in series.

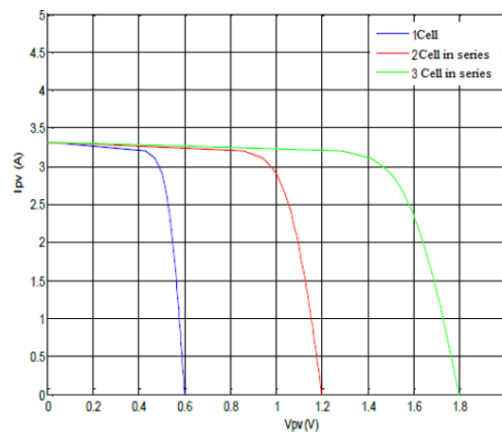


Figure I-12: I-V characteristic of cells connected in series.

I.5.2 The cells in parallel association

The characteristics of cells connected in parallel are equivalent to those connected in series. This implies that when cells are connected in parallel, they experience the same voltage, and the features of the group can be obtained by combining the currents at a particular voltage. By connecting N_p (V_{co} , I_{cc}) cells in parallel (designated as index p), the resulting characteristics (V_{pco} , I_{pcc}) are demonstrated in (**Figure I-14**). [24]

$$I_{pcc} = N_p \times I_{cc} \quad \text{And} \quad V_{pco} = V_{co} \quad (\text{I-4})$$

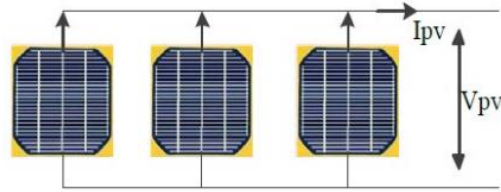


Figure I-13: Diagram of cells connected in parallel.

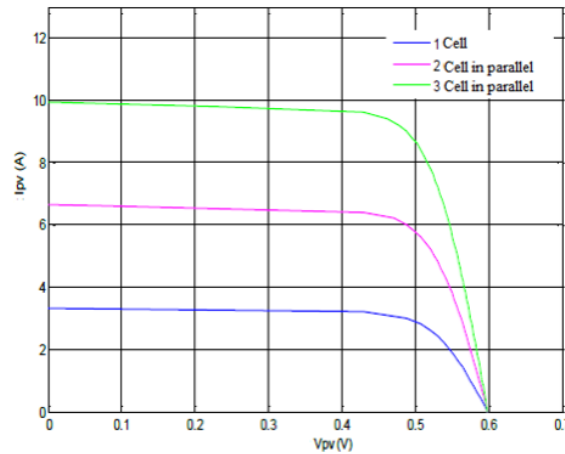


Figure I-14: I-V characteristic of cells connected in parallel.

I.5.3 The Photovoltaic effect

The initial demonstration of a solar cell utilizing the photovoltaic effect was given by Edmond Becquerel, a French scientist. Becquerel noticed that exposure to sunlight resulted in a change in electrical voltage in a material [25].

Afterward, Albert Einstein found out during his research on the photoelectric effect that light possessed not just wave-like characteristics but that its energy was transmitted by particles known as photons. The energy of a photon (E) is given by the relationship:

$$E = \frac{hc}{\lambda} \quad (\text{I-5})$$

h = Planck's constant.

C = the speed of light.

λ = the wavelength.

In 1955, a team of American researchers from Bell Telephone Laboratories (currently known as Alcatel-Lucent Bell Labs) created a photovoltaic cell that had a high energy output

of 6%. Three years later, the first solar-powered spacecraft was launched into space. Even today, satellites still rely solely on photovoltaic solar energy as their primary power source [26].

At present, the photovoltaic effect is the sole available method for producing electricity that doesn't rely on mechanical force. All other techniques, whether renewable or not, necessitate the use of rotating generators such as alternators or dynamos. These generators can be set in motion by different methods, such as steam, wind, or water power.

I.5.4 The Photovoltaic conversion

The process of converting solar energy into electrical energy is achieved through the use of semiconductor materials which contain positive P and negative N electric charges. These materials, including silicon or those coated with a thin metal layer, have the ability to release electrons when exposed to an external energy source, which is known as the photovoltaic effect. The n-type region, which was originally doped, develops a positive charge, whereas the p-type region, which was originally doped, develops a negative charge. This creates an electric field between the two regions that causes electrons to move to the n-region and holes to move to the p-region. As a result, a P-N junction is created. When metal contacts are added to the n and p-regions, a diode is formed. When the junction is exposed to light, photons carrying energy equal to or greater than the band gap energy transfer their energy to the atoms. Each atom then moves an electron from the valence band to the conduction band and also leaves behind a mobile hole, which generates an electron-hole pair. If a load is connected across the cell, electrons from the n-region will move through the external circuit to the p-region, which creates a potential difference [27]. (**Figure I-15**)

The source of energy comes from photons, which are constituent components of light. These photons collide with electrons and release them, leading to the generation of an electric current. The generated direct current is of micro power and is measured in peak watts (**Wp**), which can be converted into an alternating current by using an inverter.

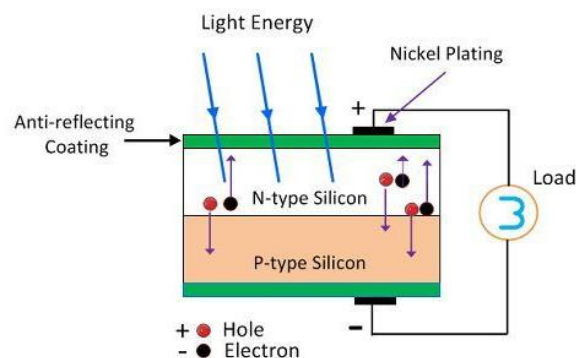


Figure I-15: Schematic presentation of a solar cell. [28]

The generated electricity can be obtained as DC power or can be stored in batteries for decentralized electrical energy, or can be fed into the grid as AC power.

I.6 The characteristics of solar cells

I.6.1 The short-circuit current density

The I_{sc} , measured in mA, is the current that passes through the cell while it is illuminated and the voltage across the cell is at zero. The amount of I_{sc} is directly proportional to the level of light received, and its value is predominantly influenced by the ability of the charge carriers to move within the cell. [29]

This means that there exists an equation that is an approximation of it: [30]

$$I_{sc} \approx \frac{I_{ph}}{1 + \frac{R_s}{R_p}} \quad (\text{I-6})$$

R_s : Series resistance [Ω] & R_p : Parallel resistance [Ω]

In the ideal case ($R_s \rightarrow 0$ and $R_p \rightarrow \infty$), we will have:

$$R_p \gg R_s \Rightarrow \frac{R_s}{R_p} \ll 1 \Rightarrow 1 + \frac{R_s}{R_p} = 1 \quad (\text{I-7})$$

In the ideal case, the short-circuit current then coincides with the photocurrent: $I_{sc} = I_{ph}$.

I.6.2 The open circuit voltage

The voltage that is measured when there is no electrical current passing through the cell is known as the open circuit voltage, V_{oc} . The term "open circuit" signifies that there is no flow of electrical current within the cell, resulting in a power of zero. The V_{oc} is measured in volts [29]. Its equation is: [30]

$$V_{oc} = n_{id} \times U_{th} \times \ln \left(1 + \frac{I_{ph}}{I_s} \right) \quad (\text{I-8})$$

n : The ideality factor of the diode.

I.6.3 The fill factor

The fill factor (FF) is an indicator to rely on to define the quality of a PV cell; the closer this factor is to 1, the better the cell is. FF is the ratio between the maximum powers (P_{MP}) that the cell can deliver ($I_{MP} \cdot V_{MP}$) and the power formed by the product of ($I_{SC} \cdot V_{OC}$) [31].

$$FF = \frac{P_{MP}}{I_{SC} \times V_{OC}} = \frac{I_{MP} \times V_{MP}}{I_{SC} \times V_{OC}} \quad (\text{I-9})$$

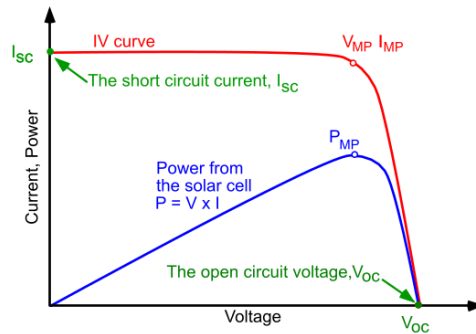


Figure I-16: Current voltage (IV) cure of a solar cell. [32].

I.6.4 The conversion efficiency

The efficiency (η) of a PV cell, expressed as a percentage, refers to the power conversion efficiency. It is defined as the ratio of the maximum power delivered by the cell to the incident power, P_{in} [30] [33]

$$\eta = \frac{P_{\max}}{P_{in}} = \frac{FF \times I_{sc} \times V_{oc}}{P_{in}} \quad (\text{I-10})$$

The performance of a cell can be enhanced by boosting the fill factor, short-circuit current, and open-circuit voltage. It's important to note that this particular parameter is crucial since it enables us to assess the cell's efficiency.

I.7 The types of photovoltaic cells

There are several varieties of solar cells, also known as photovoltaic cells, and each kind has a distinct efficiency and cost. Despite their variations, all of them have a relatively low efficiency rate of between 8 to 23% of the energy they collect. At present, there exist three primary categories of these cells. [34]

➤ **Monocrystalline cells:**

They are a type of solar cell that is made from a single crystal structure of silicon. Due to their intricate manufacturing process, these cells have the highest efficiency rate but are also the most costly to produce.

➤ **Polycrystalline cells:**

They are made from multiple crystal structures of silicon and due to their simpler design, these cells are less costly to produce, but they have a lower efficiency rate.

➤ **Amorphous cells:**

They are also known as thin-film cells and are a type of solar cell that does not have a crystalline structure like monocrystalline or polycrystalline cells. Instead, they are made from thin layers of semiconductor materials deposited onto a substrate. Despite their low efficiency, these cells are cost-effective and require thin layers of silicon, making them suitable for small consumer products like solar-powered calculators and watches.

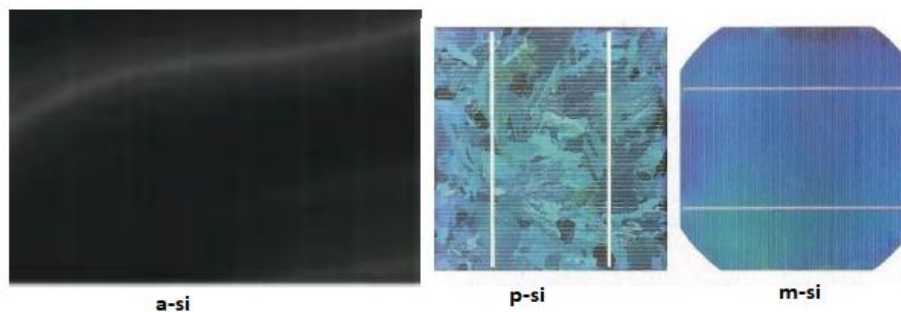


Figure I-17: Pictures depicting various kinds of photovoltaic cells

➤ **Organic Photovoltaic (OPV) Cells:**

Organic Photovoltaic (OPV) cells use organic semiconductor materials to convert sunlight into electricity. They are lightweight and flexible, but currently have lower efficiency compared to crystalline silicon cells. Research aims to enhance efficiency, stability, and commercial viability of OPV technology. [35]

➤ **Cadmium Telluride (CdTe) Cells:**

Cadmium Telluride (CdTe) cells are thin-film solar cells using cadmium and tellurium semiconductor materials. They are cost-effective with high efficiency in commercial

production. However, proper handling and recycling are essential due to cadmium's toxicity and environmental concerns. [35]

The following (**Table 1**) present the different types of cells with their efficiency:

Cell Technologies	Laboratory Efficiency	Production Efficiency
Amorphous Silicon (a-Si)	13%	5 To 9 %
Polycrystalline Silicon (p-Si)	19.8%	11 To 15 %
Monocrystalline Silicon (m-Si)	24.7%	13 To 17 %
Organic Photovoltaic (OPV) Cells	3%	2% to 8%
Cadmium Telluride (CdTe) Cells	14%	9% to 12%

Table I-1: The different types of cells with their efficiency.

I.8 Conclusion

Solar cells have the potential to revolutionize the way we generate electricity, as they provide a clean and renewable source of energy. Understanding the science behind solar cells, from the properties of the sun to the principles of semiconductors and photovoltaic conversion, is essential to harnessing the full potential of this technology.

By exploring the various types of solar cells available, we can also see how solar energy can be adapted to suit different needs and applications. With ongoing advancements and research in this field, we can look forward to a future powered by sustainable and environmentally-friendly energy sources.

The MPPT Techniques and DC-DC Converters

II.1 Introduction

The current limitations in harnessing the full potential of solar energy despite its relative abundance on Earth. Solar panels typically convert only 15-22% of solar energy into usable energy due to factors like placement, orientation, and atmospheric conditions. To address these limitations, solar trackers and Maximum Power Point Tracking (MPPT) systems are commonly used to optimize energy production. Solar trackers orient PV modules towards the sun while MPPT adjusts the duty cycle of the boost converter to maximize power output. Researchers have developed various methodologies to extract as much power as possible from PV panels, and numerous MPPT algorithms are available for both off-grid and grid-connected PV systems.

In this chapter, we will dive into the application of MPPT techniques, in particular Perturb & Observe, Incremental conductance and Particle Swarm Optimization on photovoltaic systems. Interest in these controls is increasing due to its ease of development and its wide range of uses. In automation or power electronics. All these algorithms have different characteristics regarding complexity, convergence speed, step response, steady state oscillations about MPP and required electronics equipment. The goal of these controls is to bring the operation of the system closer to the MPP by altering the duty cycle of the Boost converter.

II.2 The MPPT Solar Charge Controller

A solar charge controller equipped with an MPPT algorithm is designed to optimize the current flowing from the PV module to the battery. This is achieved through the use of a DC-DC converter topology that converts DC input from the solar panel into AC and back into a different DC voltage and current that precisely matches the PV module to the battery. Examples of DC-DC converters include the Buck and Boost converters. The main function of an MPPT solar charge controller is to maximize the amount of current going into the battery from the PV module. [36]



Figure II-1: MPPT charge Controller.

The MPPT tracking efficiency is 99%, and the power generation efficiency of the entire system can reach 97% (**Figure II-2**). Compared with the PWM controller, the MPPT can improve the control accuracy and the output power of the solar panel can be increased by 5%-30%.

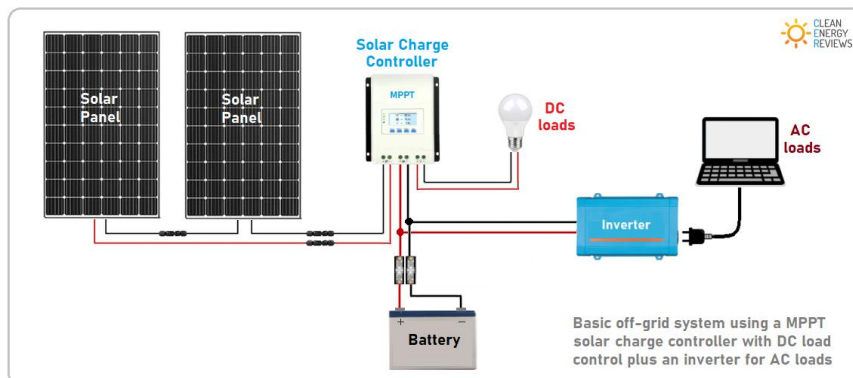


Figure II-2: Chain diagram of an MPPT controlled solar panel.

II.2.1 The DC-DC Converter

Choppers, also known as DC-DC converters, are devices that enable precise regulation of electrical power in DC circuits with exceptional flexibility and efficiency. A chopper comprises capacitors, inductors, and a switch. In an ideal scenario, these components do not consume any active power, resulting in the attainment of high efficiencies in choppers.

There are several types of DC-DC converters, with all falling under non-isolated and isolated converters. Non-isolated converters, such as buck, boost, and buck-boost converters, have a direct electrical connection between the input and output sides, while isolated converters, such as fly back and forward converters, use a transformer to provide galvanic isolation between the input and output. [37]

DC-DC converters are controlled by PWM, in which a high frequency pulse signal is used to turn the electronic switches between the ON and OFF state, thus controlling the converter voltage. There are numerous types of conversion techniques, including magnetic, capacitive electronic, linear, switched mode, and more.

The converter and MPPT system are located inside a MPPT Solar Charge Controller and are linked to the PV module as shown below (**Figure II-3**)

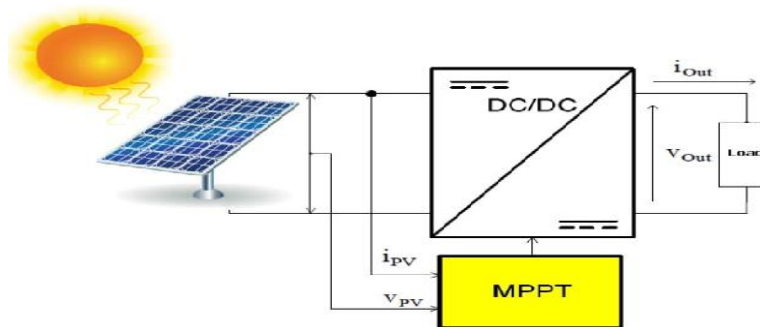


Figure II-3: DC-DC converter in PV system [38]

DC-DC converters play a crucial role in PV systems because they match the voltage output of the PV modules to the voltage requirements of the load or the grid. They are also important in enabling the implementation of MPPTs and this allows for efficient energy conversion and improved overall system performance.

II.2.2 The Boost Converter

A Boost converter, sometimes referred to as a Step-Up Converter, is a specific type of switched mode power supply designed to increase a DC voltage to a higher level. It performs the function of converting a lower DC voltage into a higher DC voltage. This versatile converter is commonly employed as a source-load adapter in scenarios where the operating point, in direct coupling (**Figure II-3**), is situated to the right of the Maximum Power Point (MPP).

Using the diagram below (**Figure II-4**) as a guide, we can see how the components are connected in this instance. The input voltage supply is connected to the associated inductance, followed by the solid-state device that serves as a switch, which is connected across the supply. The load and the capacitor are connected in parallel and both in series with the diode. [39]

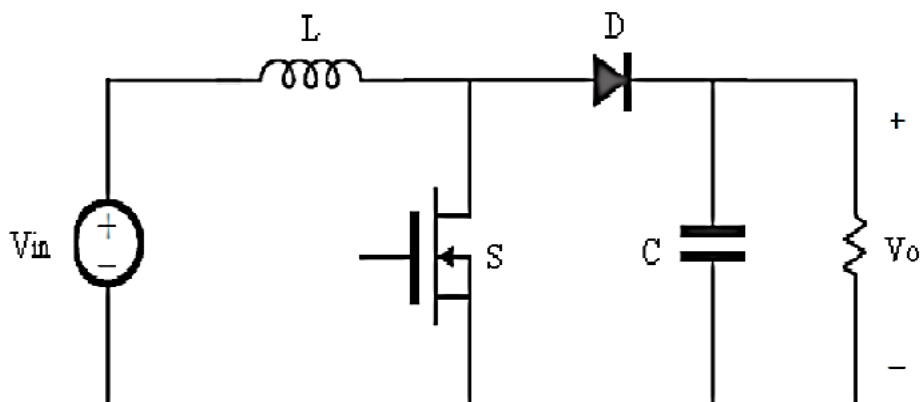


Figure II-4: Circuit diagram of a Boost converter.

The boost converter has two modes of operation that are mode switch **ON** and mode switch **OFF**.

- During the mode switch ON, Diode is OFF:

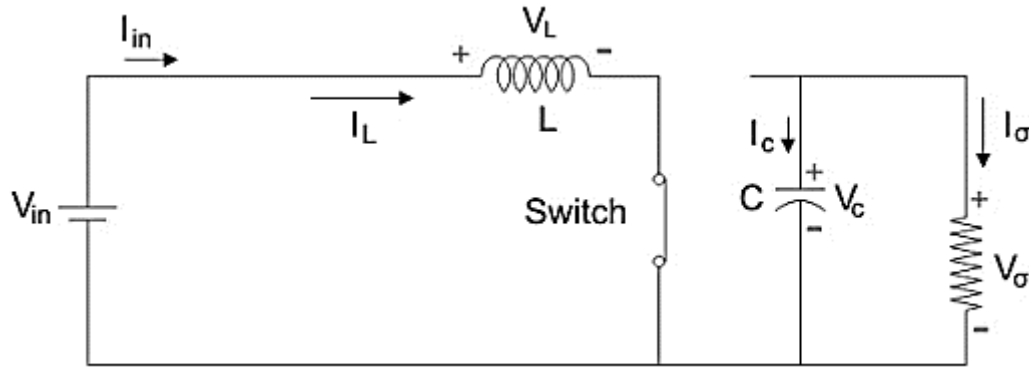


Figure II-5: Boost converter with switch ON and diode OFF.

The term "Switch ON mode" describes the state of the switch being turned on, which creates a short circuit. This state is designed to provide minimal resistance, allowing current to flow without hindrance. Consequently, when the switch is on, all the current will pass through it and return to the direct current (DC) input source.

We assume that the switch is on for a time T_{ON} and is off for a time T_{OFF} . Henceforth we define the time period, T , as:

$$T = T_{ON} + T_{OFF} \quad (\text{II-1})$$

Giving us the switching frequency as:

$$f = \frac{1}{T} \quad (\text{II-2})$$

We can also define the duty cycle given as:

$$D = \frac{T_{ON}}{T} \quad (\text{II-3})$$

By applying Kirchhoff's Voltage Law, we examine the Boost converter during steady-state operation:

$$V_{in} = V_L \quad (\text{II-4})$$

$$V_L = L \frac{di_L}{dt} = V_{in} \quad (\text{II-5})$$

$$\frac{di_L}{dt} = \frac{\Delta i_L}{\Delta t} = \frac{\Delta i_L}{DT} = \frac{V_{in}}{L} \quad (\text{II-6})$$

As the switch is closed for a certain period of time $T_{ON} = DT$ (Equation II-3) we can then say that $\Delta t = DT$ and we substitute into (Equation II-6 to get Equation II-7).

$$\left(\Delta i_L\right)_{closed} = \left(\frac{V_{in}}{L}\right)DT \quad (\text{II-7})$$

During the analysis of the Boost converter, it is important to consider the following key points:

- Ensuring continuous current flow through the inductor by selecting an appropriate value for L.
- Observing that during the ON state, the current through the inductor steadily rises from a positive slope to reach a maximum value, and then decreases back to its initial value with a negative slope. As a result, the overall change in the inductor current over a complete cycle is zero.

During the mode switch OFF, Diode is ON:

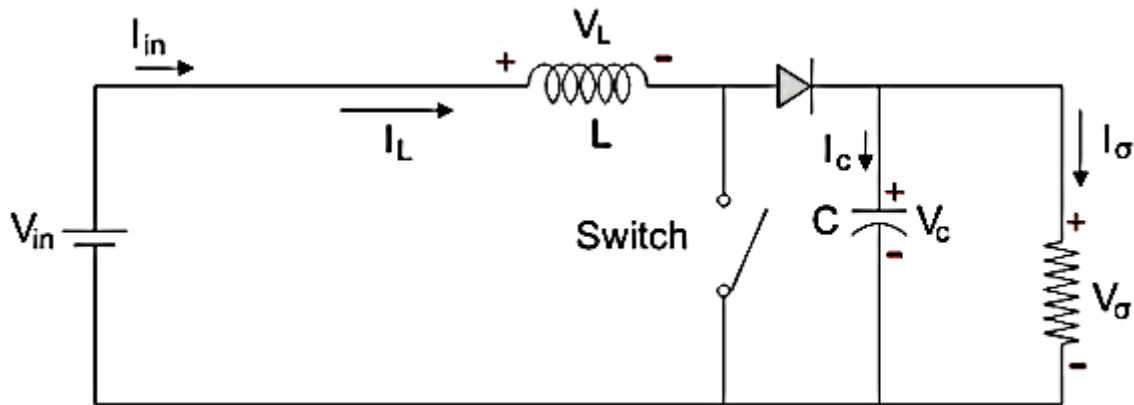


Figure II-6: Boost converter when switch is OFF and diode is ON

During this mode, the inductor's polarity is reversed, releasing stored energy that is dissipated in the load resistance. This aids the current flow in the load and raises the output voltage as the inductor acts as a source in conjunction with the input source. However, for analysis purposes, the original conventions and Kirchhoff's Voltage Law are maintained. [39]

In the second mode and using Kirchhoff's Voltage Law, we analyze the Boost converter in steady space operation:

$$V_{in} = V_L + V_O \quad (\text{II-8})$$

$$V_L = L \frac{di_L}{dt} = V_{in} - V_O \quad (\text{II-9})$$

$$\frac{di_L}{dt} = \frac{\Delta i_L}{\Delta t} = \frac{\Delta i_L}{(1-D)L} = \frac{V_{in} - V_O}{L} \quad (\text{II-10})$$

Since the switch is open for a certain amount of time

$$T_{OFF} = T - T_{ON} = T - DT = (1-D)T \quad (\text{II-11})$$

We can therefore say

$$\Delta t = (1-D)T \quad (\text{II-12})$$

$$(\Delta i_L)_{open} = \left(\frac{V_{in} - V_O}{L} \right) (1-D)T \quad (\text{II-13})$$

It has previously been determined that the overall change in the inductor current over a complete cycle is zero

$$\left(\frac{V_{in} - V_O}{L} \right) (\Delta i_L)_{closed} + (\Delta i_L)_{open} = 0 \quad (\text{II-14})$$

$$(1-D)T + \left(\frac{V_O}{L} \right) DT = 0 \quad (\text{II-15})$$

$$\frac{V_O}{V_{in}} = \frac{1}{1-D} \quad (\text{II-16})$$

When implementing boost converters in PV systems the input voltage and output voltage are shown below: [40]

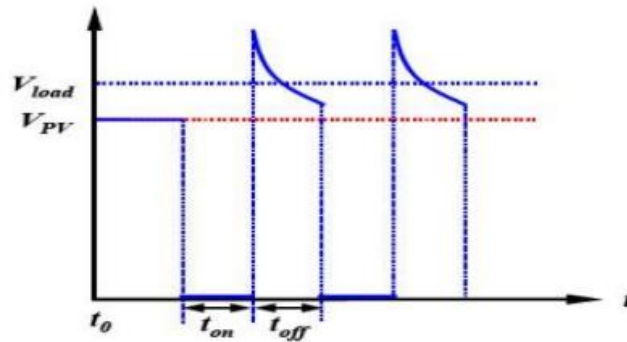


Figure II-7: Voltage waveforms of V_{pv} and V_{load} when considering a Boost converter.

(Figure II-7) represents the waveform of the load voltage. The purpose of diode D is to prevent the discharge of capacitor C when the switch is activated. It is assumed that the capacitor is adequately sized to effectively smooth out the load voltage. The load voltage waveform is determined by:

$$V_{load} = \frac{T}{t_{off}} V_{pv} = \frac{1}{1-D} V_{pv} \quad (\text{II-17})$$

With:

$D = \frac{t_{on}}{T}$: represents the duty cycle ($0 < D < 1$).

We are only focusing on the circuit's behavior when it is in a state of continuous conduction.

II.3 The Maximum Power Point (MPP)

The maximum power point (MPP) is the point on an I-V curve where a solar PV device generates the highest power output, which is determined by the product of current intensity (I) and voltage (V). This point represents the optimal bias potential where the solar cell outputs the maximum net power. The MPP voltage may vary due to factors such as irradiance intensity, device temperature, and device degradation. To maximize net power output, PV module engineering involves the development of systems that continuously track the MPP over time.

MPPT (Maximum Power Point Tracking) is a technique or algorithm used to extract the maximum power from photovoltaic modules by continuously determining the point of highest power output under varying solar radiation, ambient temperature and solar cell temperature. An effective (MPP) tracking (MPPT) system should also account for unforeseen events like imperfect operating conditions and individual cell failures. [41]

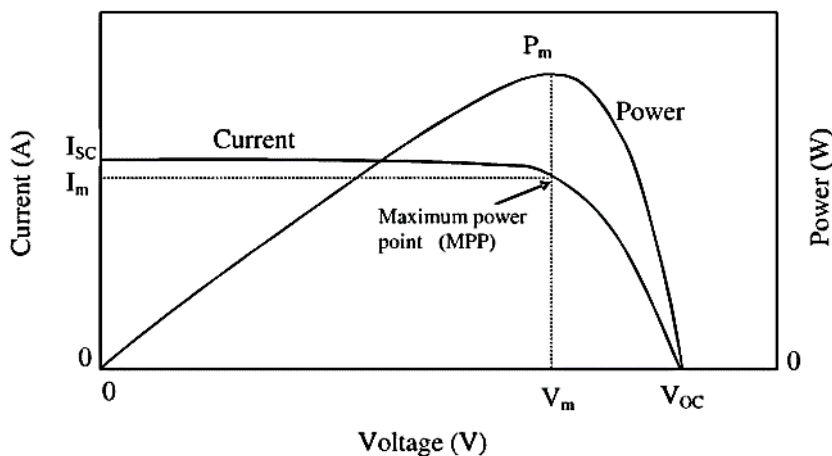


Figure II-8: MPP on I-V and P-V curves.

II.4 The various algorithms used for MPPT

In this dissertation we have been tasked to focus on only three MPPT techniques whose working principles and algorithms are explained below. These techniques are:

II.4.1 Perturb and Observe (P&O)

II.4.1.1 Principle

Several researchers have explored this simple strategy that has gained popularity for commercial PV modules due to its ease of implementation and cost-effectiveness. The perturb and observe (P&O), as the name itself states that the algorithm is based on the observation of the array output power and on the perturbation (increment or decrement) of the power based on increments of the array voltage or current. The algorithm continuously increments or decrements the reference current or voltage based on the value of the previous power sample.

The P&O algorithm states that when the operating voltage of the PV panel is perturbed by a small increment, if the resulting changes in power ΔP is positive, then we are going in the direction of MPP and we keep on perturbing in the same direction. If ΔP is negative, we are going away from the direction of MPP and the sign of perturbation supplied has to be changed [42].

In P&O, steady-state oscillation occurs because perturbations continuously change. Until reaching the MPP, this situation is recapitulated. The MPP is achieved when the changes of power with respect to changes in voltage being zero ($\frac{dP}{dV} = 0$). If the value of the present power $P(t)$ of the panel is larger than its previous value $P(t-1)$ then we keep the same direction of disturbance, if not, it reverses the disturbance of the previous cycle. In simple terms, the P&O algorithm states that when the operating voltage of the PV panel is perturbed by a small increment, if the resulting changes in power ΔP is positive, then we are going in the direction of MPP and we keep on perturbing in the same direction. If ΔP is negative, we are going away from the direction of MPP and the sign of perturbation supplied has to be changed. [43]

II.4.1.2 Algorithm

The algorithm compares the power and voltages of time (k) with the previous sample at a time (t-1) and predicts the time to approach to MPP. A small voltage perturbation changes the power of the solar panel if the power alteration is positive, voltage perturbation is continued in the same track but if power change (dP or ΔP) is negative, it indicates that the MPP is far away and the perturbation is decreased to reach the MPP.

Table 1 shows the summary of the P&O algorithm. Thus, in this way the whole PV curve is checked by small perturbations to find the MPP that increases the response time of the algorithm. [44]

Present perturbation (dV)	Change in power (dP)	Next perturbation direction
$dV > 0$	$dP > 0$	Positive
$dV > 0$	$dP < 0$	Negative
$dV < 0$	$dP > 0$	Negative
$dV < 0$	$dP < 0$	Positive

Table II-1: Summary of Perturb and observe algorithm.

The dynamic response of the P&O method is slow, especially when low sampling rates and small value increments are used. This is because the P&O method tends to oscillate the operating point near the MPP, and using low increments is required to decrease steady-state errors. However, this slows down the algorithm. To speed up the algorithm, a higher sampling rate may be employed, but this comes with the tradeoff of choosing a lower increment value. Therefore, there is a need for a tradeoff between the increment and the sampling rate in the P&O method to achieve satisfactory results. [45]

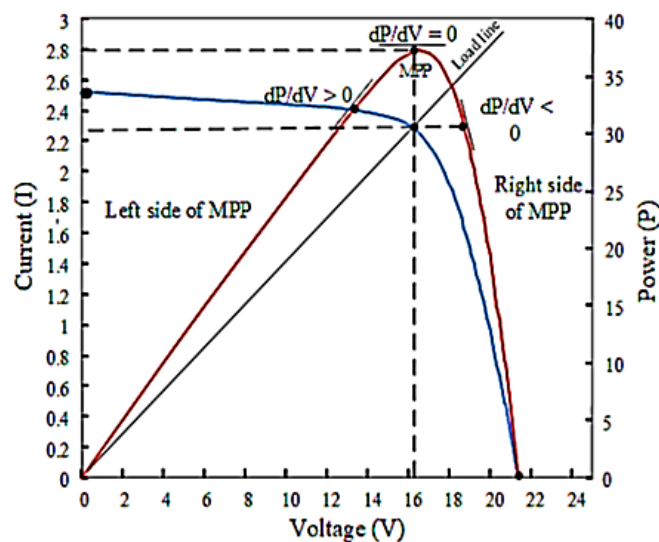


Figure II-9: Operating characteristic of P&O method. [43]

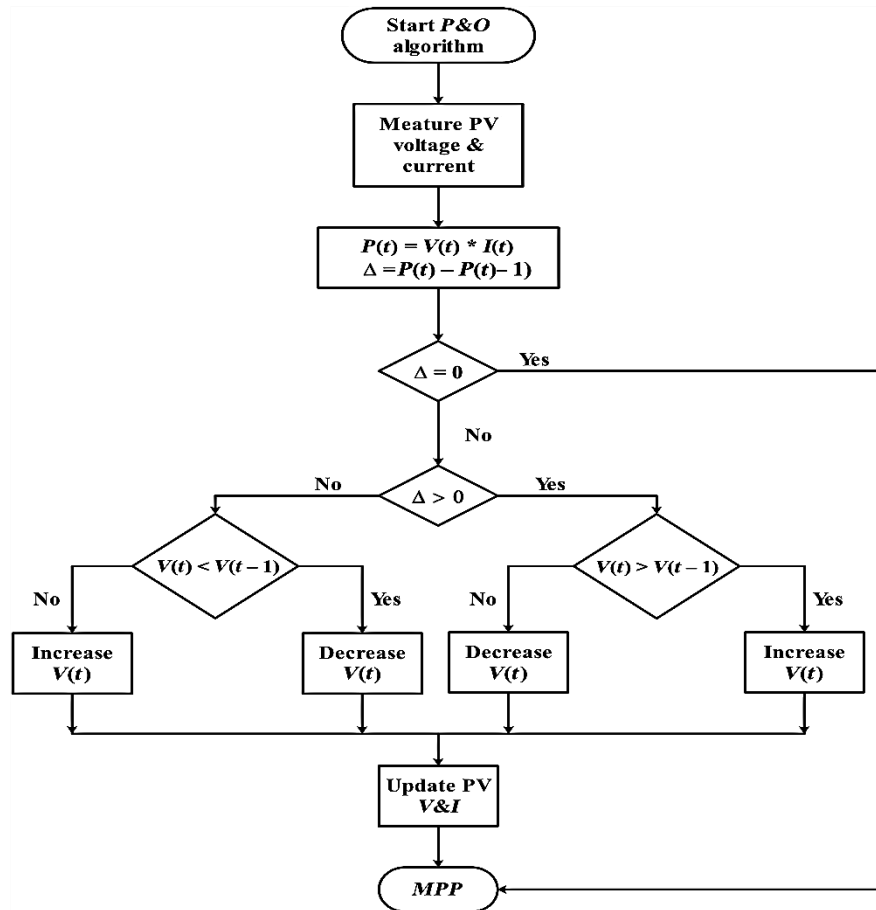


Figure II-10: Algorithm for P&O

II.4.1.3 Advantages and disadvantages of P&O [46]

➤ **Advantages:**

- Easy to implement: P&O is relatively simple compared to other MPPT methods, making it easier to incorporate into PV systems.
- Good performance under uniform radiation: P&O provides accurate and efficient tracking of the maximum power point under stable environmental conditions.

➤ **Disadvantages:**

- When using a small increment value and low sampling rate, the P&O method has a slow dynamic response. To reduce steady-state errors, it is necessary to use small increments as the P&O method tends to oscillate the operating point near the MPP. A lower increment value will bring the system closer to the array MPP, while a higher increment value will result in faster algorithm performance but increased steady-state error. To achieve a satisfactory steady-state error, a low increment value is necessary. However, this slows down the algorithm, so a higher sampling rate may be employed to increase the algorithm speed. There is, therefore, a need to find a balance between the increment and the sampling rate in the P&O method.

- In P&O algorithms, a common issue is that the array terminal voltage is perturbed every cycle of the MPPT process. As a result, when the MPP is reached, the output power oscillates around the maximum value, leading to power loss in the PV system. This problem is more pronounced when there are constant or slowly changing atmospheric conditions.
- The oscillation around the PPM under normal operating conditions. It should be noted that these oscillations can be reduced if we set a low incrimination step but at the expense of convergence time. So, a compromise must be made between accuracy and speed. when choosing this

The poor convergence of the algorithm in the case of sudden variations of the temperature and/or sunlight.

II.4.2 Particle swam optimization PSO

II.4.2.1 Principle

The Particle Swarm Optimization (PSO) algorithm, developed by R. Eberhard and J. Kennedy in 1995, is a simple bio-inspired technique used for solving nonlinear optimization problems. PSO is a type of artificial intelligence optimization method that imitates the social behavior of flocks of birds, swarms of bees, or schools of fish searching for food. This optimization algorithm is widely used by researchers in academia and industry due to its simple algorithm structure and fast convergence rates, which are controlled by a few parameters. PSO operates on two fundamental principles, which involve learning from previous data and sharing current information among swarm agents.

Two important rules are applied on these swarm agents. Let us call these agents as particles then:

Rule 1: All particles should follow that particle whose performance is best.

Rule 2: all particles should move towards that particle having best condition.

The particles in the PSO algorithm continue to move towards the optimal result until the termination criterion is satisfied. It is important to note that the velocity and position of the best particle are used as a reference for all other particles, which move in the direction of the global particle fitness to reach the optimal solution. [47], [48]

The velocity and position updating used in conventional PSO can be mathematically represented as,

$$v_i^{k+1} = wv_i^k + c_1r_1x(P_{best} - s_i^k) + c_2r_2x(G_{best} - s_i^k) \quad (\text{II-18})$$

$$s_i^{k+1} = s_i^k + v_i^{k+1} \quad (\text{II-19})$$

Where:

v_i^k is the particle velocity at iteration k ,

w is the inertia weight factor

c_1 and c_2 are called acceleration constants,

r_1 and r_2 are random numbers and

s_i^k is the particle position in the search space at iteration k

P_{best} is called local best and G_{best} is called global best.

Each iteration of the inertia weight value is updated through the following equation:

$$w = w_{\max} - \frac{w_{\max} - w_{\min}}{iter_{\max}} x(iter) \quad (\text{II-20})$$

II.4.2.2 Algorithm

Firstly, initialize the particles randomly in the search space where early velocities for the particles are chosen arbitrarily and particle positions are determined. Then, the fitness of each particle is evaluated by contributing single particle elucidation to objective function. The computed fitness values are compared against the previous values for updating the individual personal and global best. Their corresponding positions are also updated accordingly. Then the velocity along with the position of every particle is modernized. Check for the convergence criterion and stop the procedure if it satisfied. Else, increment iteration count and repeat the process as shown in the figure below. [47] For the MPPT system based on the PSO algorithm designed, the particle position is determined as the duty cycle that will be given to the DC-DC converter and particle speed is set as a change in duty cycle, while the evaluation function of the fitness value or objective function is chosen as the maximum power generated in PV (Figure II-11) depicts the flow chart of the PSO method. [48]

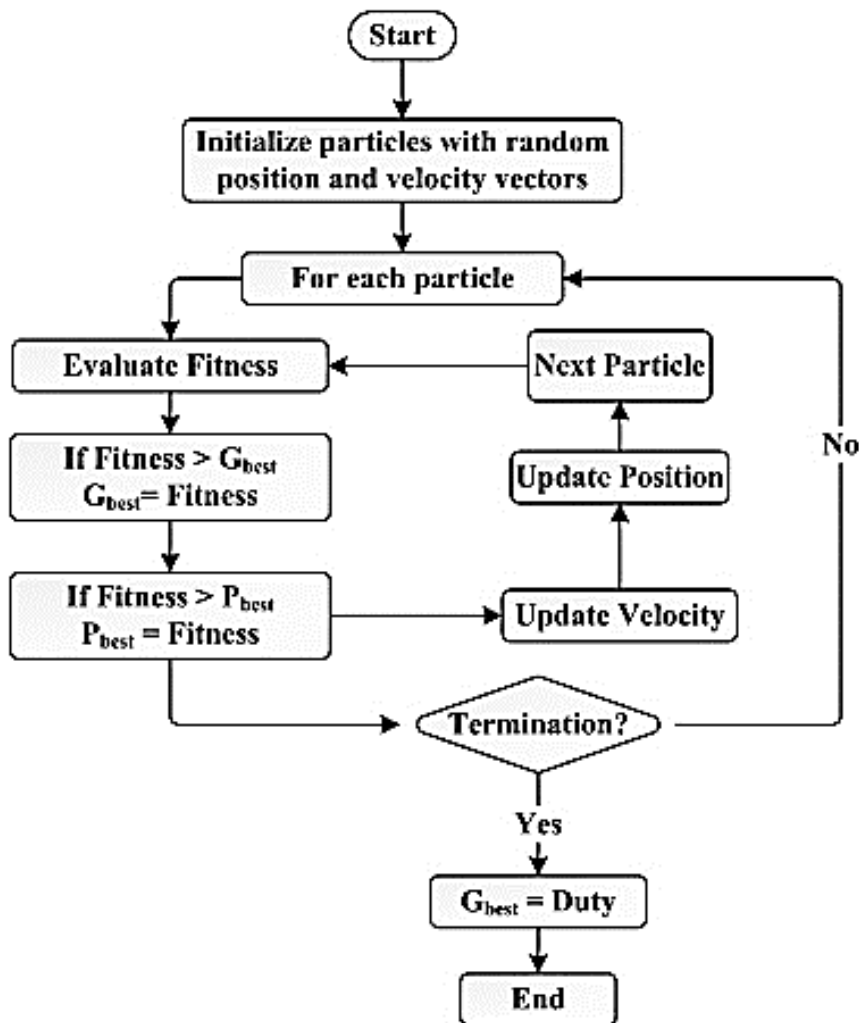


Figure II-11: PSO flowchart

II.4.2.3 Advantages and disadvantages of PSO [49]

➤ Advantages:

- High convergence speed and high precision.
- Accurate tracking of the maximum power point (MPP).
- Highly improved performance of the PV plants.

➤ Disadvantages:

- Slow speed of convergence.
- Large search space.
- Very complex method of MPPT.

II.4.3 Incremental Conductance

II.4.3.1 Principle

The principle of the conventional incremental conductance algorithm is based on comparing the value between the derivative of current in the function of voltage and the PV array instantaneous current against voltage. This algorithm simply tracks the MPP by increasing or decreasing the reference voltage based on the operating point of the system. At MPP, the following conditions must be met: [50]

$$\frac{dP}{dV} = 0 \quad (\text{II-21})$$

$$\frac{dP}{dV} = \frac{d(V.I)}{dV} = I + V \frac{dI}{dV} \quad (\text{II-22})$$

$$\frac{dI}{dV} = -\frac{I}{V} \quad (\text{II-23})$$

Where:

$\frac{dI}{dV}$: The derivation of current in the function of voltage.

$\frac{I}{V}$: The PV instantaneous current against voltage.

Mode	Perturbation	MPP Level	Status
Mode-1	$\frac{dP}{dV} = 0 \quad \frac{\Delta I}{\Delta V} = -\frac{I}{V}$	At MPP	Hold $V_{pv} = V_{mpp}$
Mode-2	$\frac{dP}{dV} > 0 \quad \frac{\Delta I}{\Delta V} > -\frac{I}{V}$	The left side of MPP	Increase voltage until $V_{pv} = V_{mpp}$
Mode-3	$\frac{dP}{dV} < 0 \quad \frac{\Delta I}{\Delta V} < -\frac{I}{V}$	Right side of MPP	Decrease the voltage until $V_{pv} = V_{mpp}$

Table II-2: Summary of Incremental Conductance algorithm.

II.4.3.2 Algorithm

By comparing the conductance and the increment of the conductance, three positions of the functioning point can be distinguished:

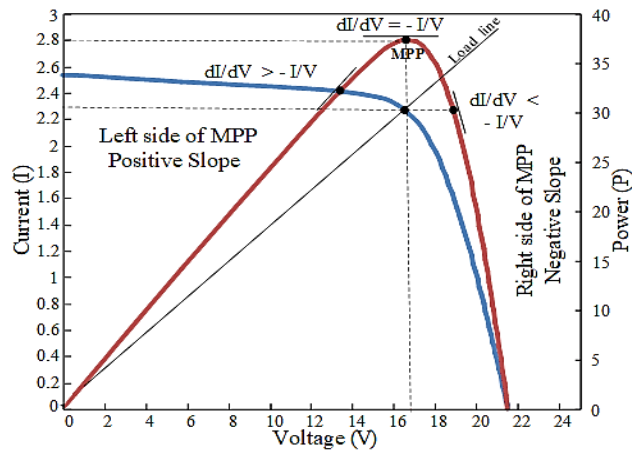


Figure II-12: Operating characteristic of incremental conductance method.

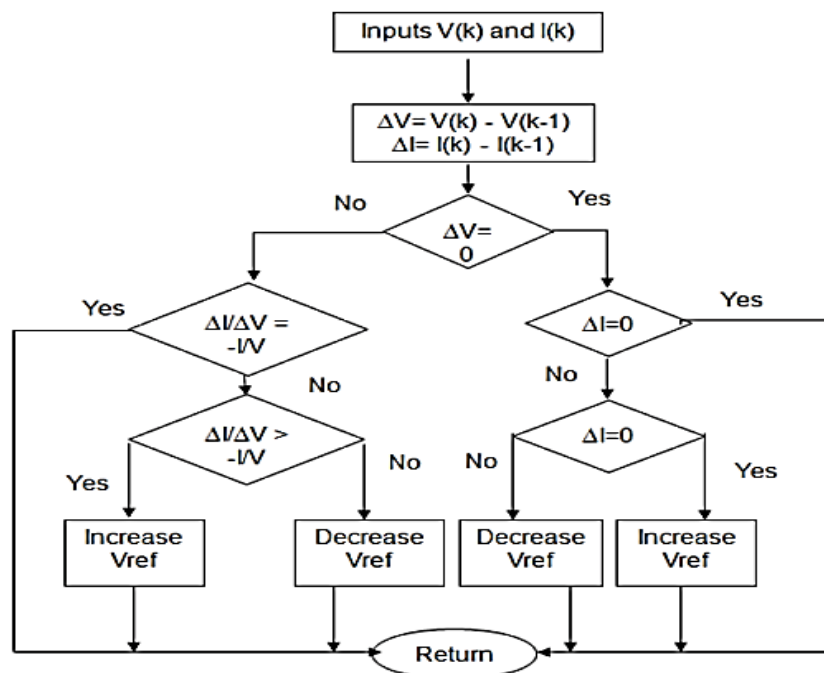


Figure II-13: Algorithm for Incremental Conductance [51]

II.4.3.3 Advantages and disadvantages of IC [52] [53]

➤ Advantages:

- Can track rapidly increasing and decreasing irradiance conditions with high accuracy.
- Can improve the response speed of the system.

➤ Disadvantages:

- More complex when compared to perturb and observe method.
- Slightly harder to implement than perturb and observe method.

II.5 Conclusion

In conclusion, the second chapter of our study focused on MPPT (Maximum Power Point Tracking) technology and its crucial role in maximizing the energy output of solar panels. We presented MPPT solar charge controllers and explained the concept of maximum power point (MPP), and reviewed three MPPT algorithms: perturbation and observation (P&O), particle swarm optimization (PSO), and incremental conductance.

Our analysis suggests that the selection of an appropriate MPPT algorithm depends on the specific application, and each algorithm has its strengths and weaknesses. Therefore, further research is necessary to enhance the efficiency and reliability of MPPT algorithms and to promote the affordability and accessibility of solar power.

Simulation and Results

III.1 Introduction

In this last chapter, we will present a prescribed photovoltaic system while implementing different methods of maximum power point tracking by using a MATLAB tool called SIMULINK. Using SIMULINK allows us to modify the system parameters easily such as the metrological conditions, and to visualize the effect of varying temperature and irradiance on the PV system.

The performance of three different Maximum Power Point Tracking (MPPT) techniques, namely Perturb and Observe (P&O), Particle Swarm Optimization (PSO), and Incremental Conductance (IC), are compared using Simulink. The simulation is carried out on a photovoltaic (PV) system to evaluate the effectiveness of each technique in tracking the maximum power point (MPP) of the PV module. The results obtained from the simulation are presented and analyzed to determine the strengths and weaknesses of each MPPT technique. This chapter provides valuable insights into the design and selection of an appropriate MPPT algorithm for a given PV system.

III.2 The Simulation of the photovoltaic system

III.2.1 Simulation of the BOOST converter

Figure III-1 shows the BOOST converter structure used along this study, connected to a resistive load powered by input voltage $V_{in} = 30V \approx V_{mpp}$ and controlled by a PWM signal.

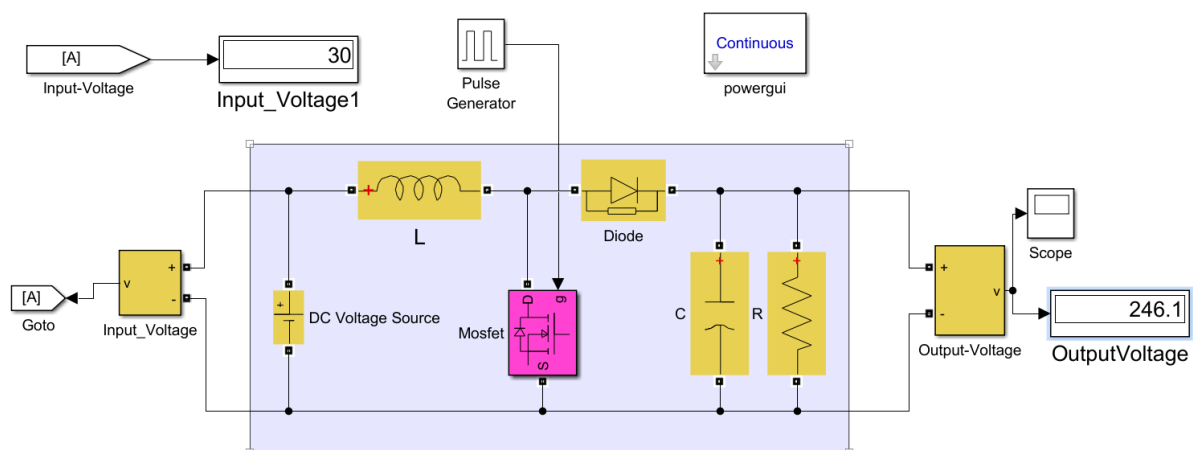


Figure III-1: The BOOST converter structure.

For our simulations require an output load voltage of around 250V and a load current of 1A, therefore calculations to determine the value of components **L**, **C1**, **R**. [54]

➤ **Inductor selection:**

$$L = \frac{V_{in} * (V_O - V_{in})}{\Delta I_L * f_s * V_O} \quad \text{(III-1)}$$

Where:

ΔI_L = estimated inductor ripple current (**30%**),

V_{in} = typical input voltage (**30V**),

V_o = desired output voltage (**250V**),

f_s = minimum switching frequency of the converter (**50kHz**),

$$L = 1.76 \times 10^{-3} \text{H}$$

➤ **Capacitor selection:**

The minimum value of output capacitor is given by

$$C = \frac{I_{out} * D}{f_s * \Delta V_O} \quad \text{(III-2)}$$

Where:

$$D = \text{duty cycle} \left[D = 1 - \frac{V_{in}}{V_o} \right]$$

I_{out} = maximum output current of the application (**1A**),

f_s = minimum switching frequency of the converter,

ΔV_o = desired output voltage ripple (**0.5%**),

$$C = 1.4 \times 10^{-5} \text{F}$$

➤ **Load Resistance:**

$$R = \frac{V_o}{I_{out}} = 250 \Omega$$

COMPONENT	VALUE
Inductor	1.76mH
Capacitor (output)	14 μ F
Capacitor (input)	0.3mF
Resistor	250 Ω
Frequency	50kHz

Table III-1: Value of components.

Boost converter results at Duty cycle=0.88

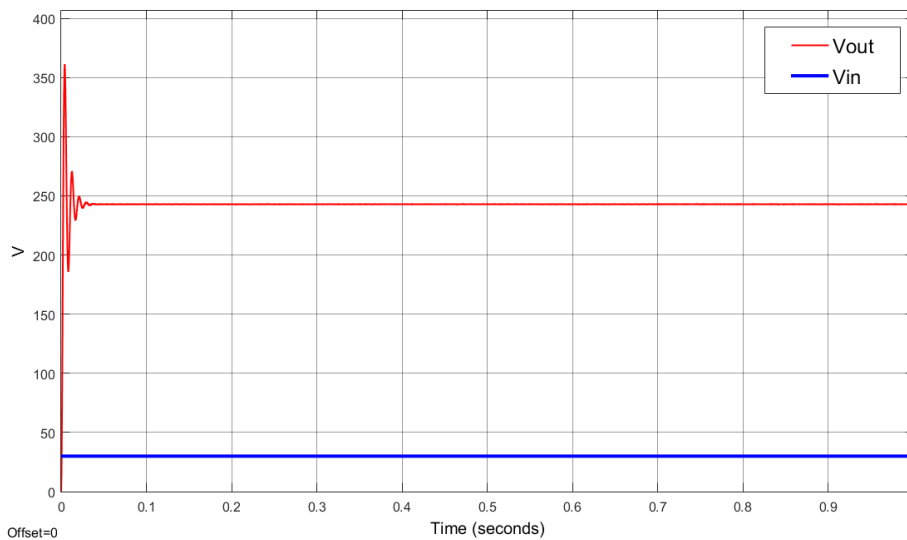


Figure III-2: Graph comparing Vin and Vout of Boost converter.

III.2.2 Simulations of the module without MPPT

In our simulations we used the **Trina Solar TSM-220PA05.08** whose parameters are shown in the figure below:

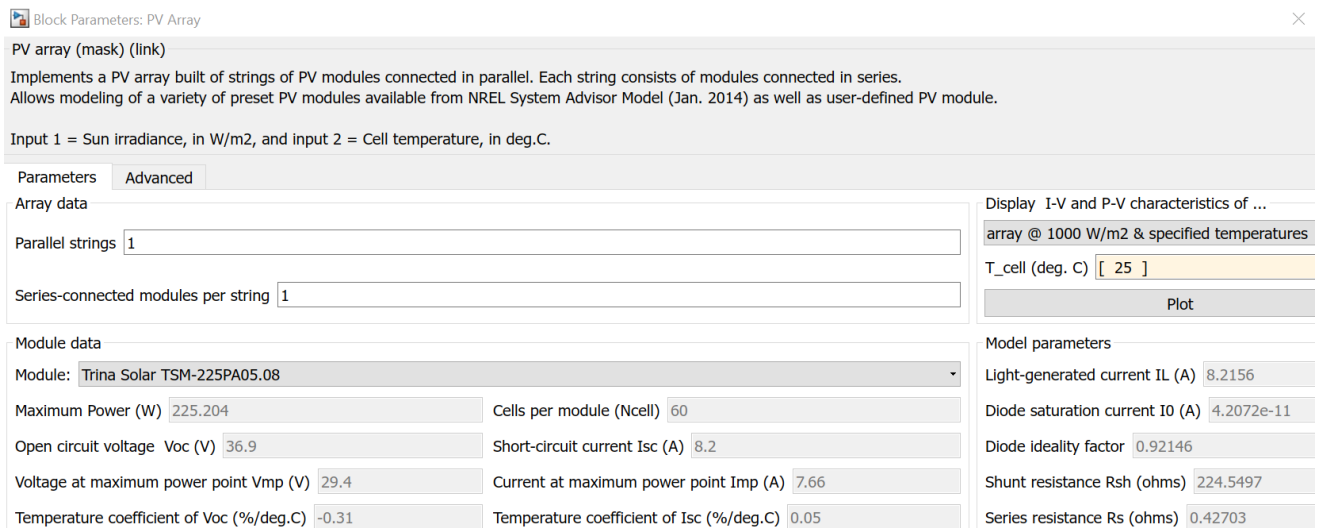


Figure III-3: PV cell parameters (Trina Solar TSM-220PA05.08).

To evaluate the performance of the selected PV panel using the studied model, a series of simulations were conducted. The figures below showcase the obtained results and provide insights into its operational characteristics.

The first curve displays the current-voltage characteristic of the PV panel under the given irradiance, while the second curve represents the power-voltage characteristic of the PV panel under the same irradiance ($G = 1000\text{W/m}^2$) and temperature ($T = 25^\circ\text{C}$).

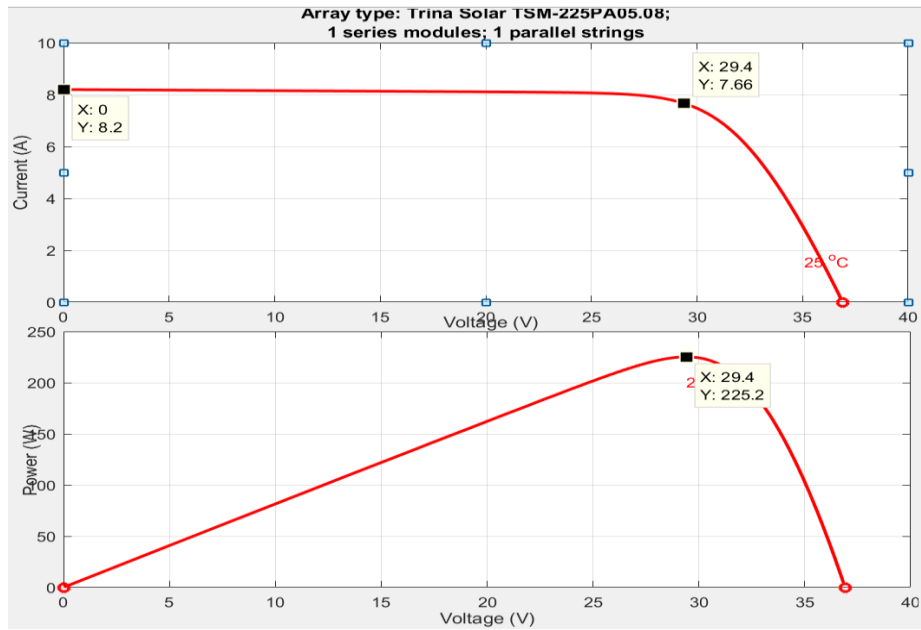


Figure III-4: IV and PV characteristic curve of the panel.

From the graphs we see that MPPT is at **P_{mpp}=225.2 W, I_{mpv}=7.66A, V_{mpv}=29.4V**
V_{oc}=36.9V, I_{sc}=8.2A.

III.2.3 Simulations with MPPT for each method at STC

Firstly, before comparing the maximization techniques, we determine the best value to use for the duty cycle step size between $\Delta\alpha = 0.001$ and $\Delta\alpha = 0.01$ using P&O algorithm

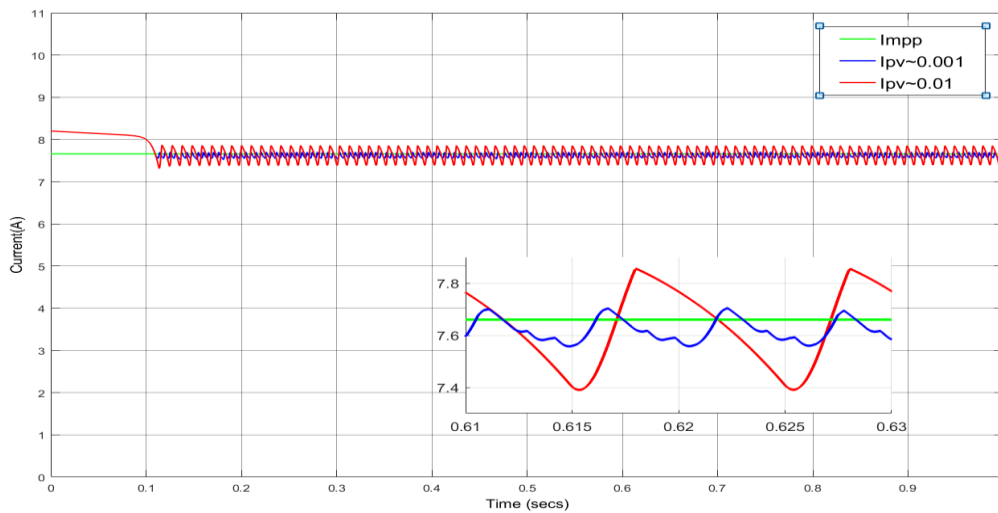


Figure III-5: PV current at $\Delta\alpha = 0.001$ and $\Delta\alpha = 0.01$.

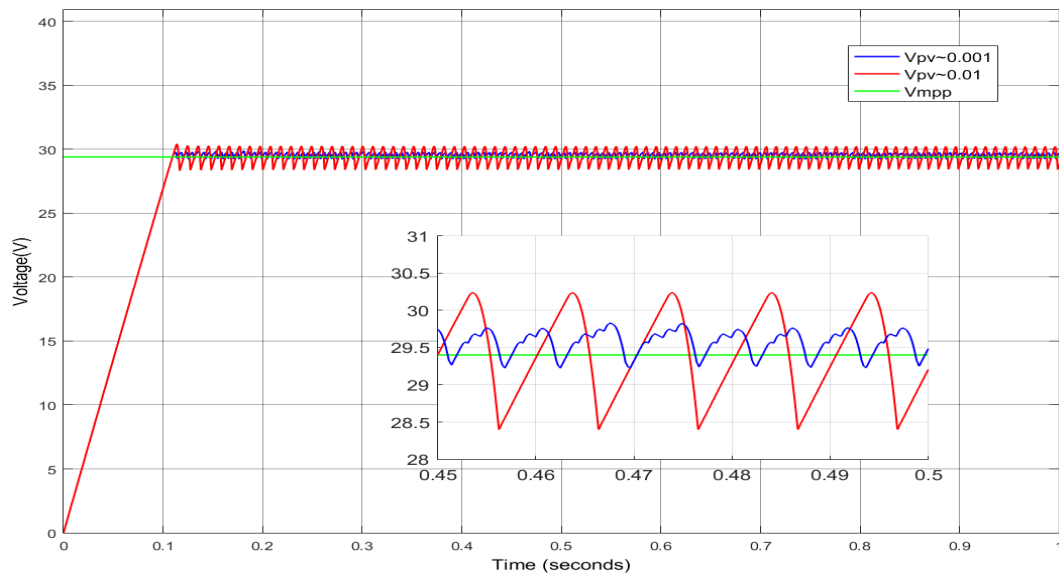


Figure III-6: PV voltage at $\Delta\alpha = 0.001$ and $\Delta\alpha = 0.01$.

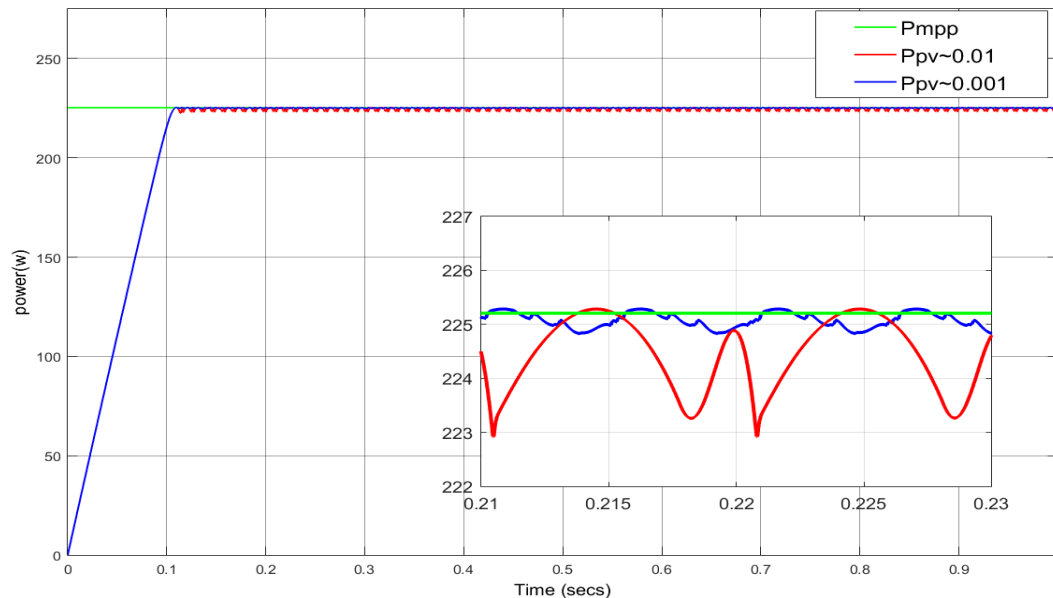


Figure III-7: PV power at $\Delta\alpha = 0.001$ and $\Delta\alpha = 0.01$.

From the graphs above, it is clear that a smaller step size allows the MPPT algorithm to approach the MPP more precisely. Consequently, the algorithm can converge to the MPP with smaller fluctuations in current, voltage and power, resulting in a smoother graphs with reduced oscillations around the MPP.

It is also notable that a larger step size can cause more significant fluctuations in power as the algorithm adjusts the operating point. This can lead to larger oscillations around the MPP on the PV power graph, potentially resulting in slower convergence to the MPP. We then decided to use a step size of 0.001 ($\Delta\alpha = 0.001$) in P&O and incremental conductance algorithms.

III.2.4 Perturb and Observe method

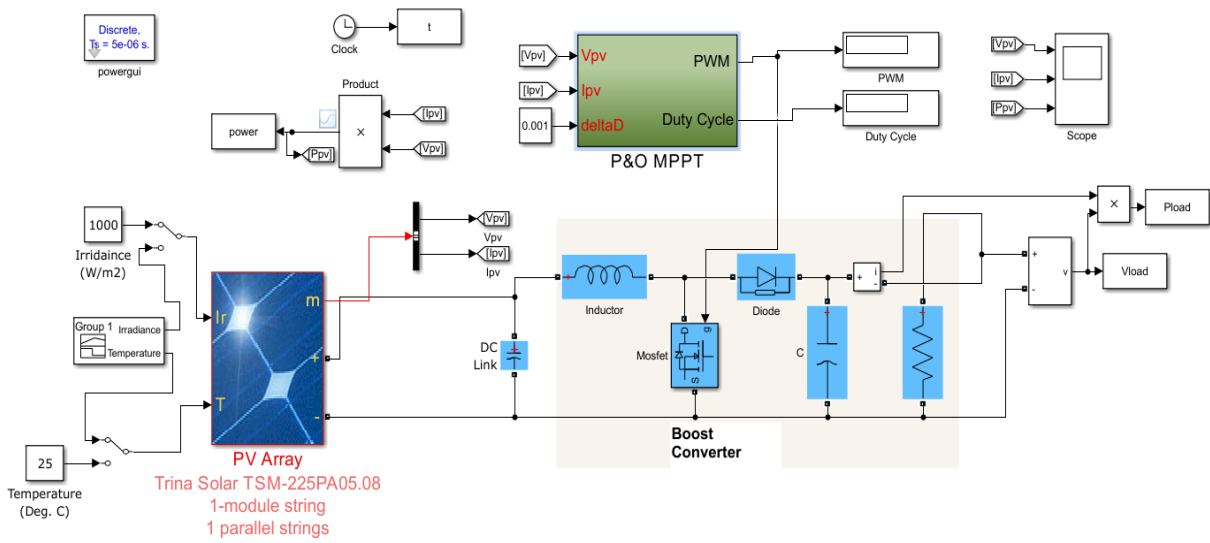


Figure III-8: Simulink diagram of a PV system using the P&O method.

- The following graphs are from the simulations:

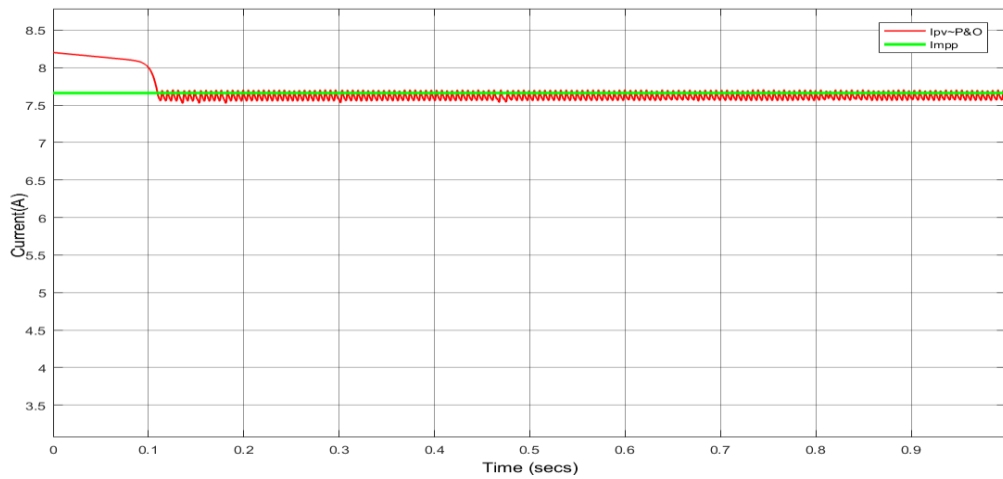


Figure III-9: PV current using the P&O method.

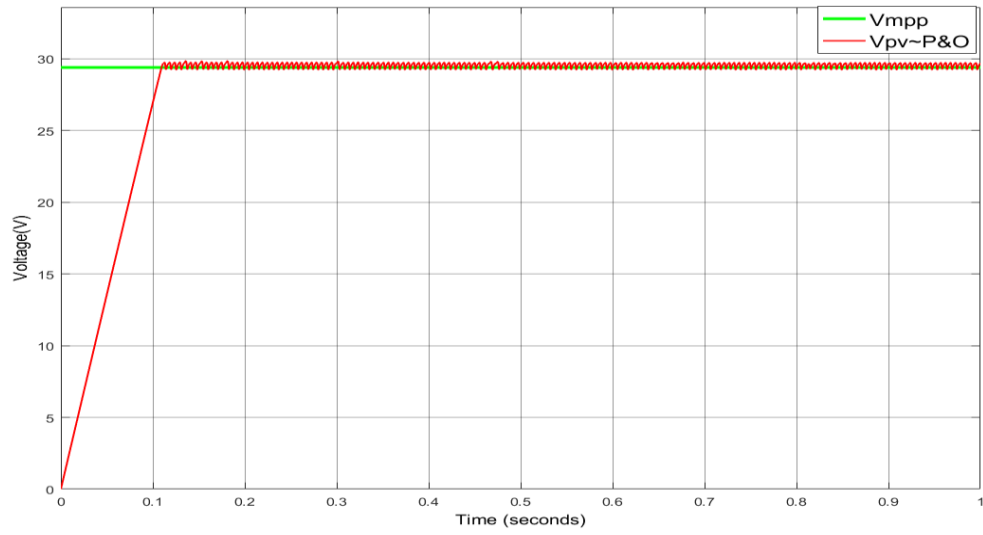


Figure III-10: PV voltage using the P&O method.

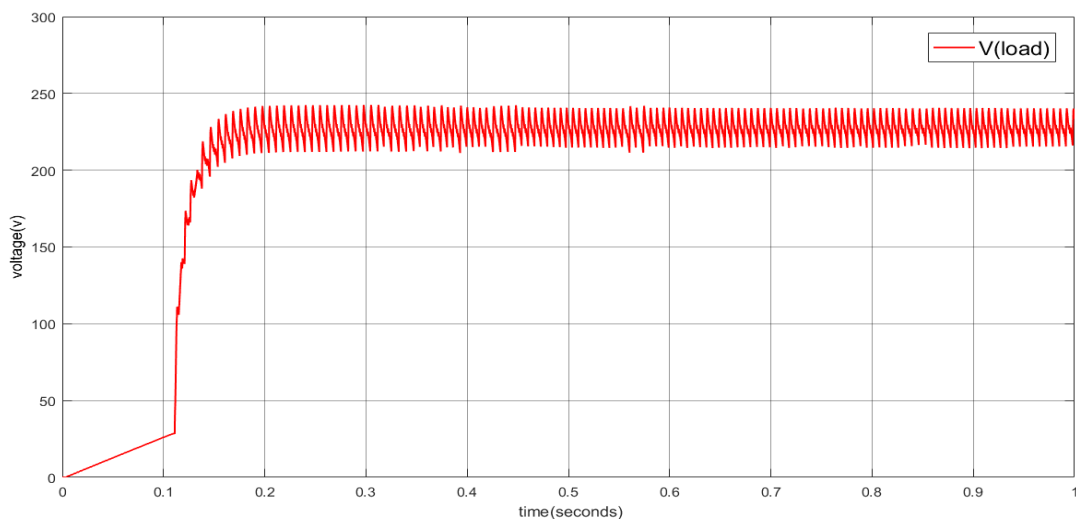


Figure III-11: Load voltage (across resistor) using the P&O method.

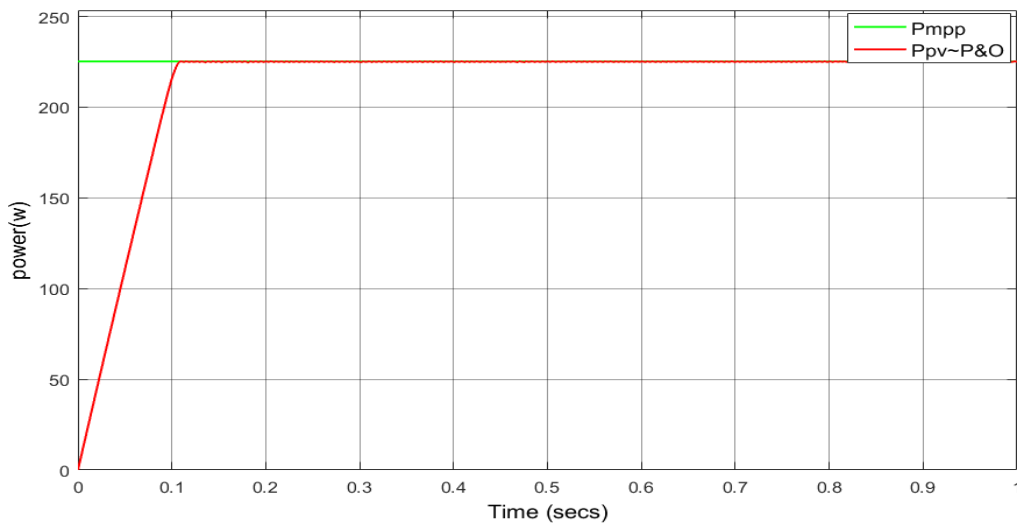


Figure III-12: PV power using the P&O method.

The PV current graph shows that the current decreases from an initial value which corresponds to the short-circuit current $I_{sc}=8.2\text{ A}$ to oscillate around a value corresponding to the maximum power point current $I_{mpp}=7.66\text{ A}$.

The PV voltage shows that the evolution of the voltage has the same behavior as the steady state power, it oscillates around a value corresponding to the voltage of the maximum power point $V_{mpp}=29.4\text{ V}$.

The load voltage graph shows that the boost converter is functioning properly as the output voltage has been boosted and oscillates around a maximum value of around 225 V .

PV power graph shows that the value of power oscillates around the value corresponding to the power at mpp of the pv module $P_{mpp}=225.2\text{ W}$.

Secondly we are also obliged to study the effect of meteorological conditions on the tracking of maximum power points (**temperature and irradiance**).

➤ Irradiance:

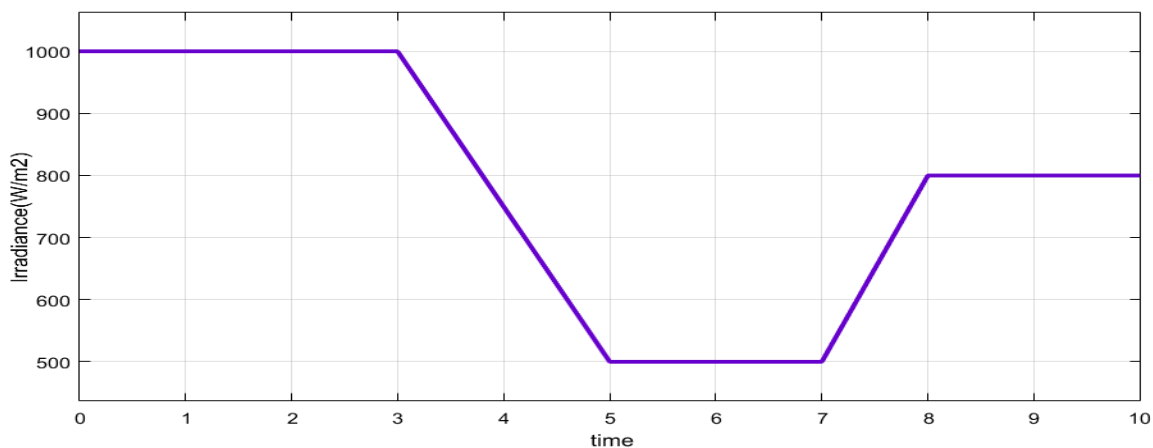


Figure III-13: Variation of irradiance with time.

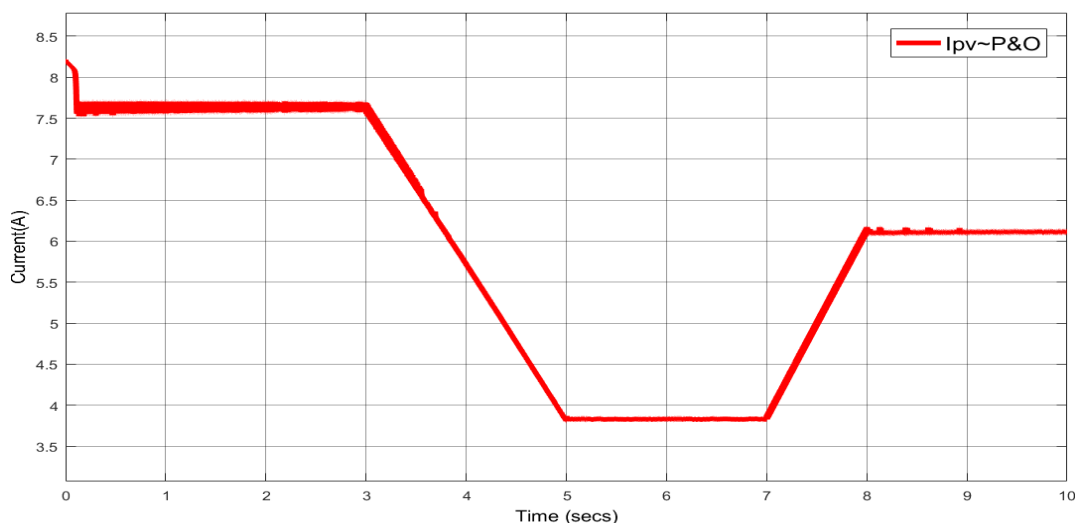


Figure III-14: Variation on I_{pv} under changing irradiance conditions.

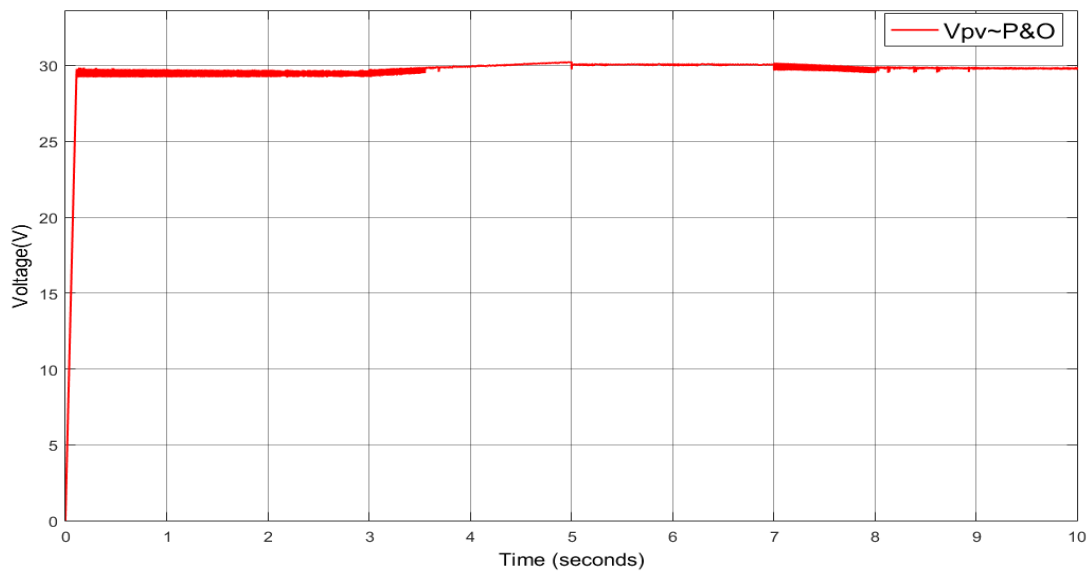


Figure III-15: Variation on V_{pv} under changing irradiance conditions.

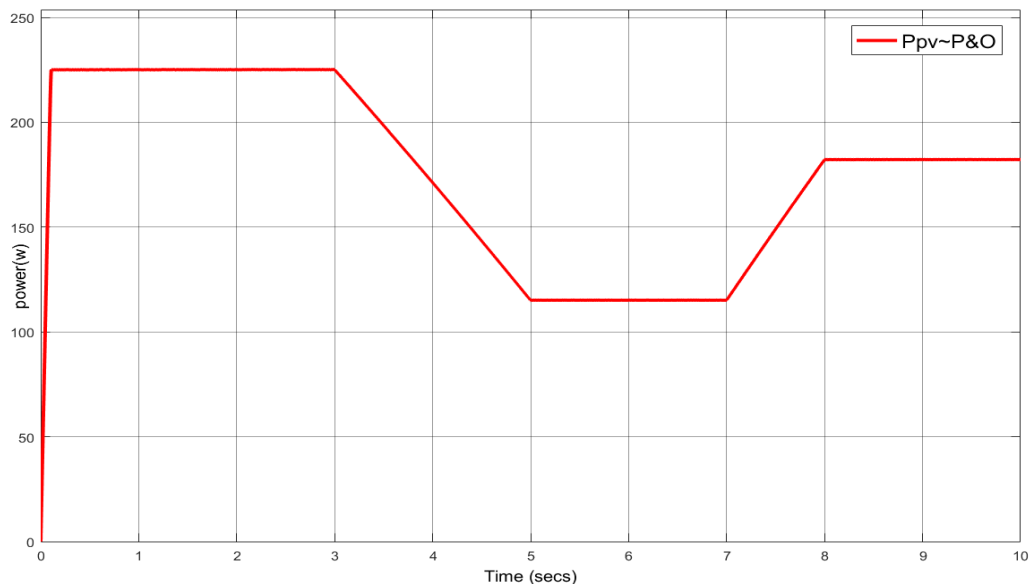


Figure III-16: Variation on P_{pv} under changing irradiance conditions.

From the simulations, we can deduce that variations in irradiance have minimum effects on PV voltage but largely have an influence on PV current.

Overall the PV power perfectly mimics the changes in irradiance levels and these two are proportional.

➤ Temperature:

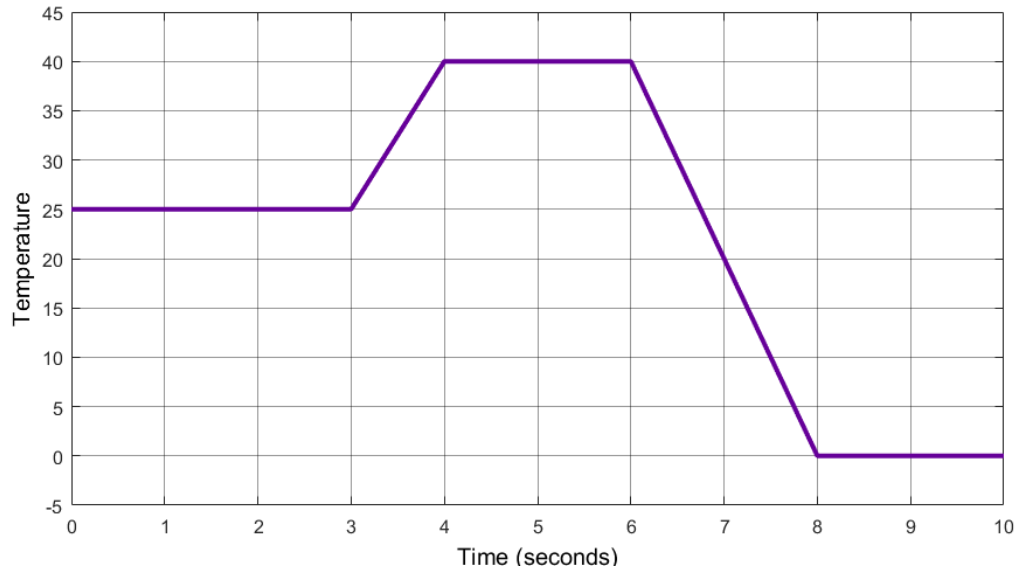


Figure III-17: Variation of temperature with time.

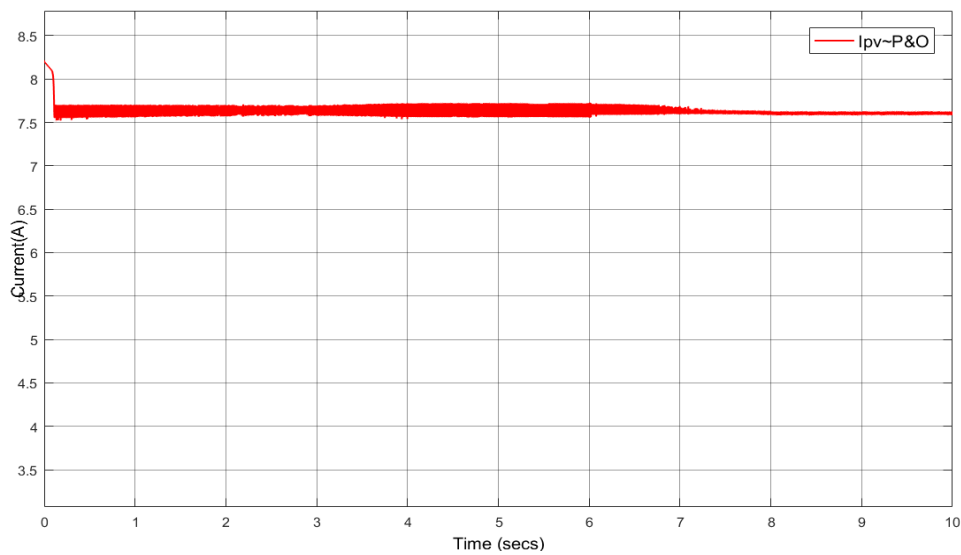


Figure III-18: Variation on I_{pv} under changing temperature conditions.

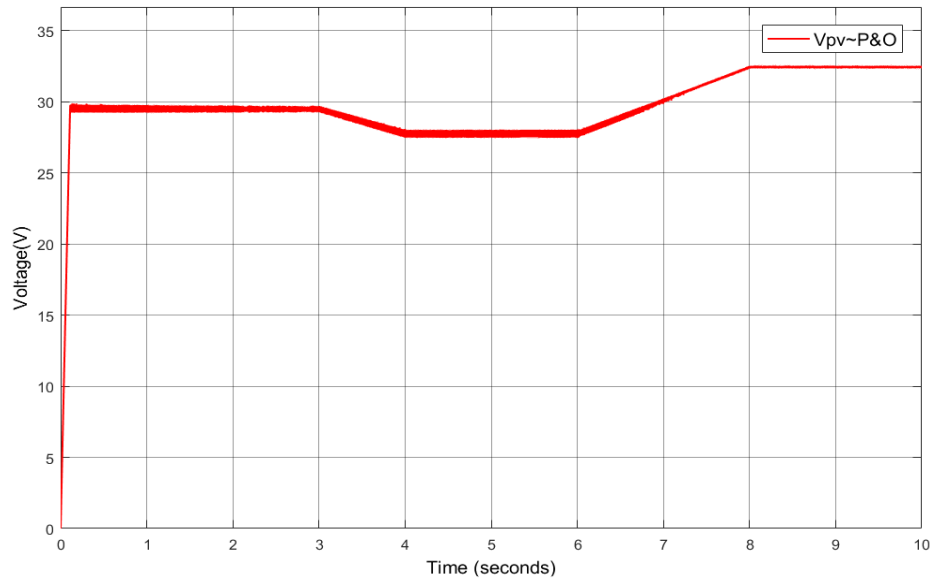


Figure III-19: Variation on V_{pv} under changing temperature conditions.

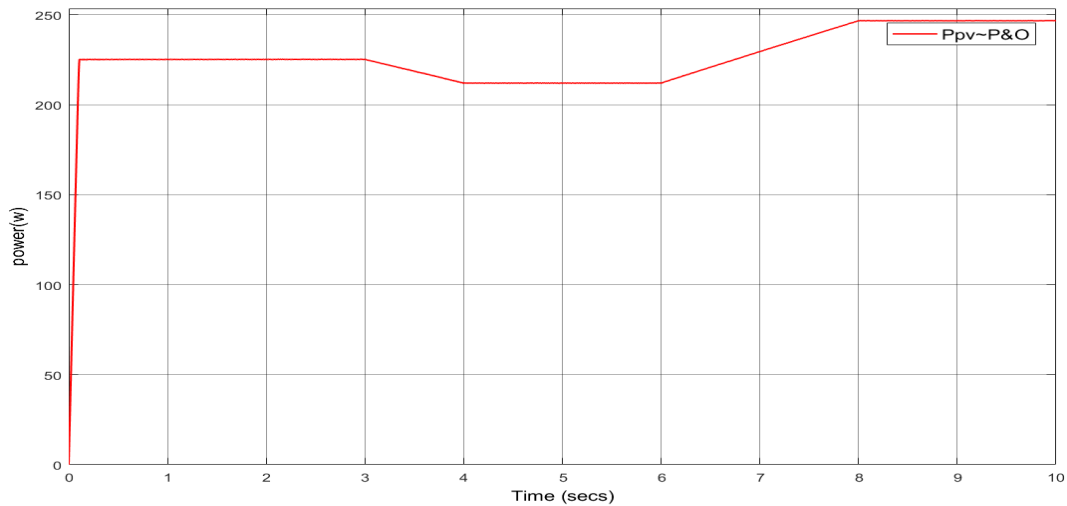


Figure III-20: Variation on P_{pv} under changing temperature conditions.

Variation From the graphs above we can conclude that PV power is inversely proportional to the temperature at a given time. The current produced by the PV module is almost constant and oscillates at around 7.66A, I_{mpp} but is more stable and smooth at lower temperatures of around 0°C.

III.2.5 Incremental Conductance Method

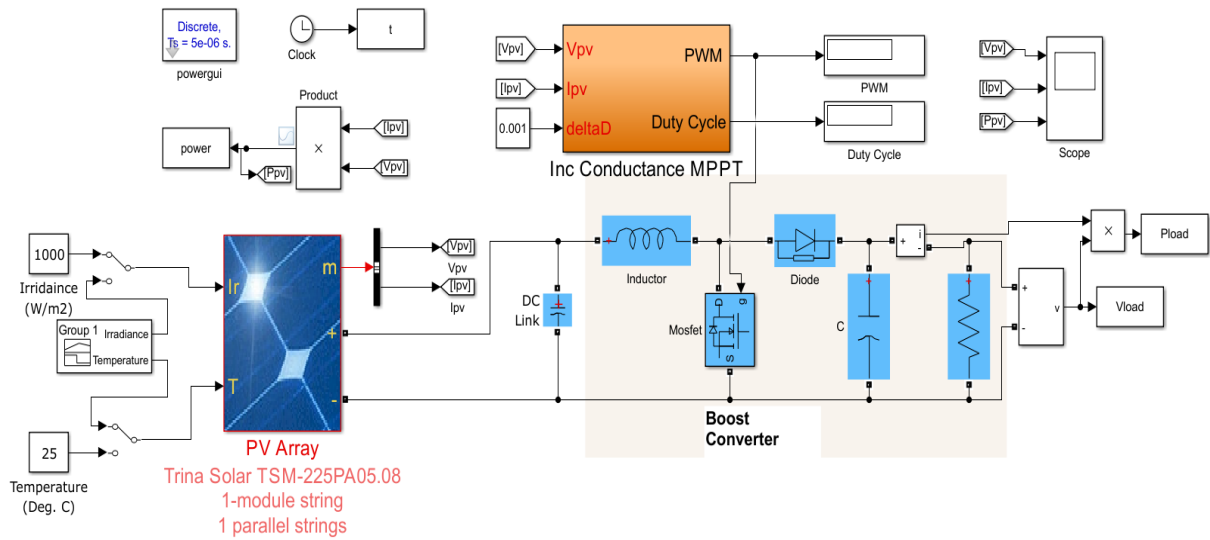


Figure III-21: Simulink diagram of a PV system with IC technique.

- The following graphs are from the simulations:

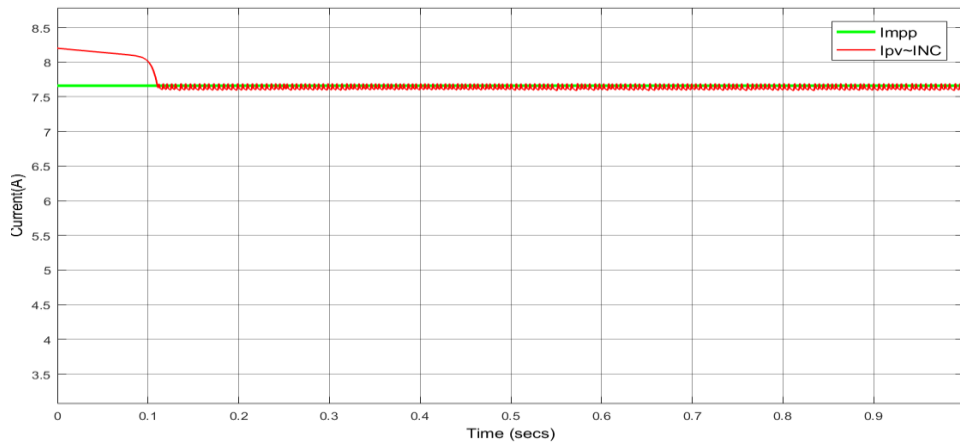


Figure III-22: PV current using the IC method.

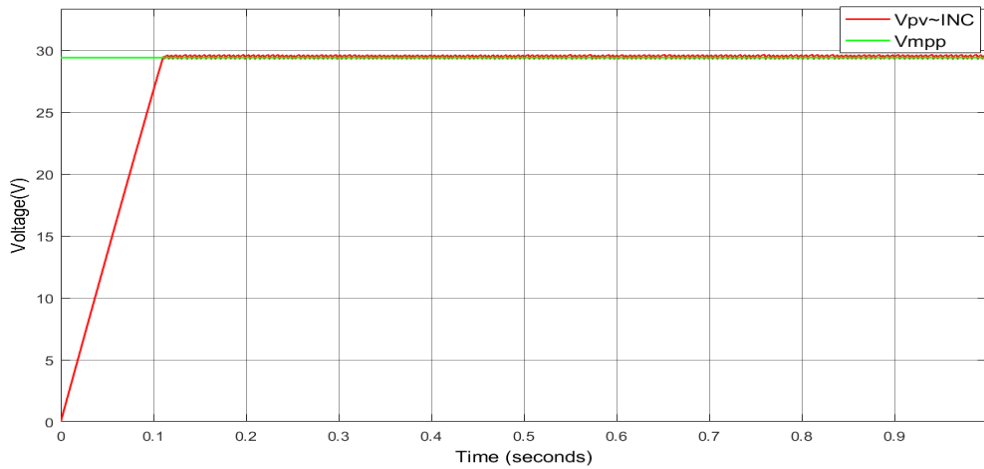


Figure III-23: PV voltage using the IC method.

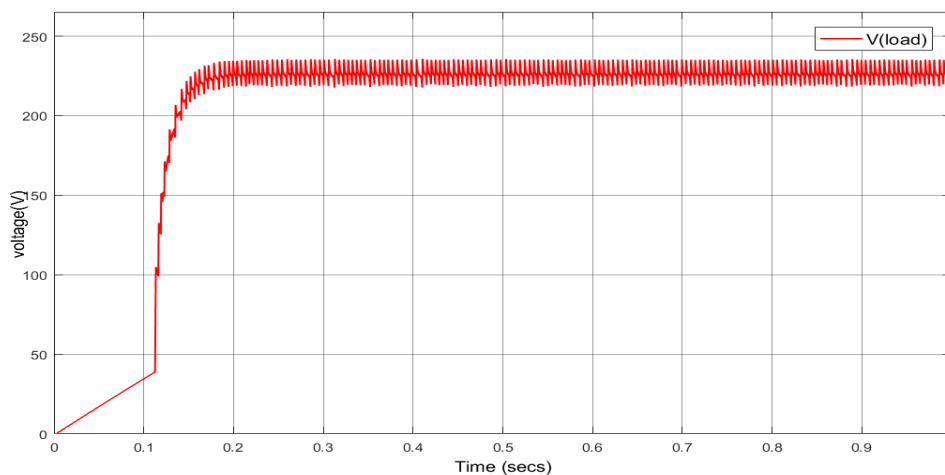


Figure III-24: Load voltage (across resistor) using the IC method.

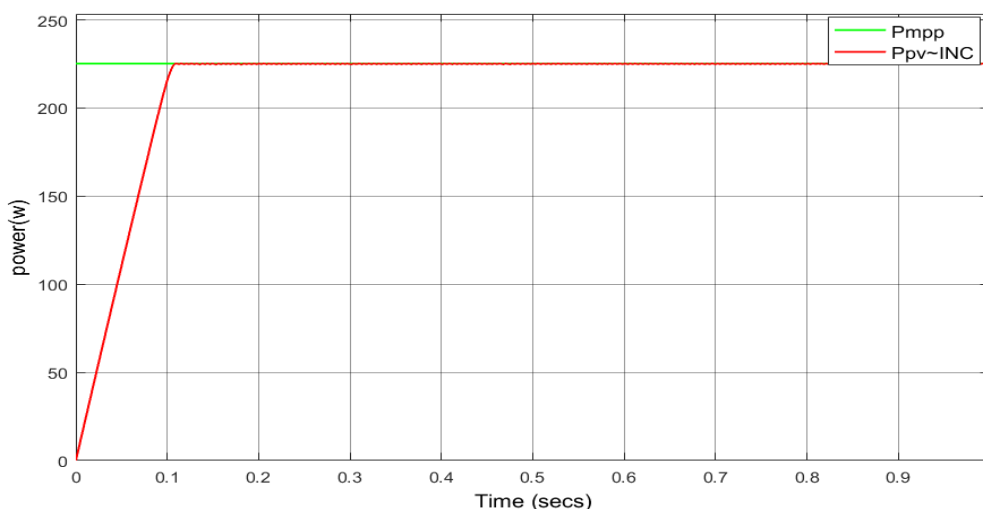


Figure III-25: PV power using the IC method.

The PV current graph shows that the current decreases from an initial value which corresponds to the short-circuit current $I_{sc}=8.2$ A to oscillate around a value corresponding to the maximum power point current $I_{mpp}=7.66$ A.

The PV voltage shows that the evolution of the voltage has the same behavior as the steady state power, it oscillates around a value corresponding to the voltage of the maximum power point $V_{mpp}=29.4$ V.

The load voltage graph shows that the boost converter is functioning properly as the output voltage has been boosted and oscillates around a maximum value of around 225V. PV power graph shows that the value of power oscillates around the value corresponding to the power at mpp of the pv module $P_{mpp}=225.2$ W.

Secondly we are also obliged to study the effect of meteorological conditions on the tracking of maximum power points (**temperature and irradiance**).

➤ Irradiance:

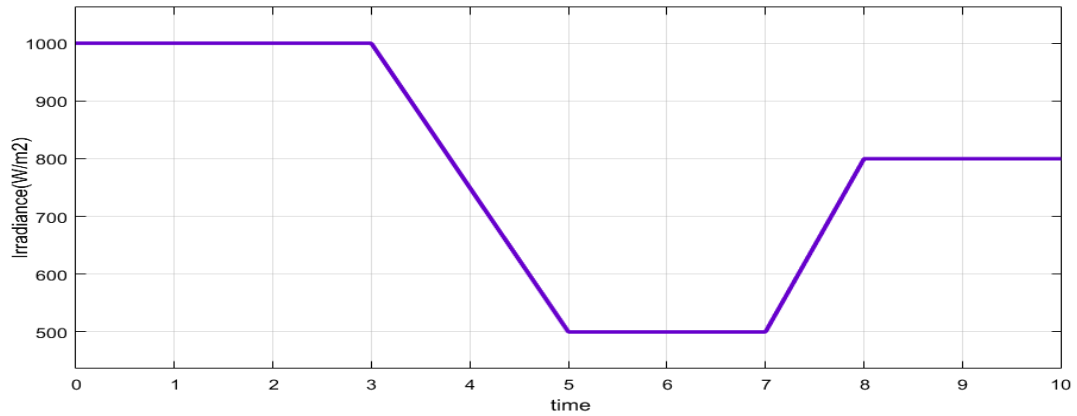


Figure III-26: Variation of irradiance with time.

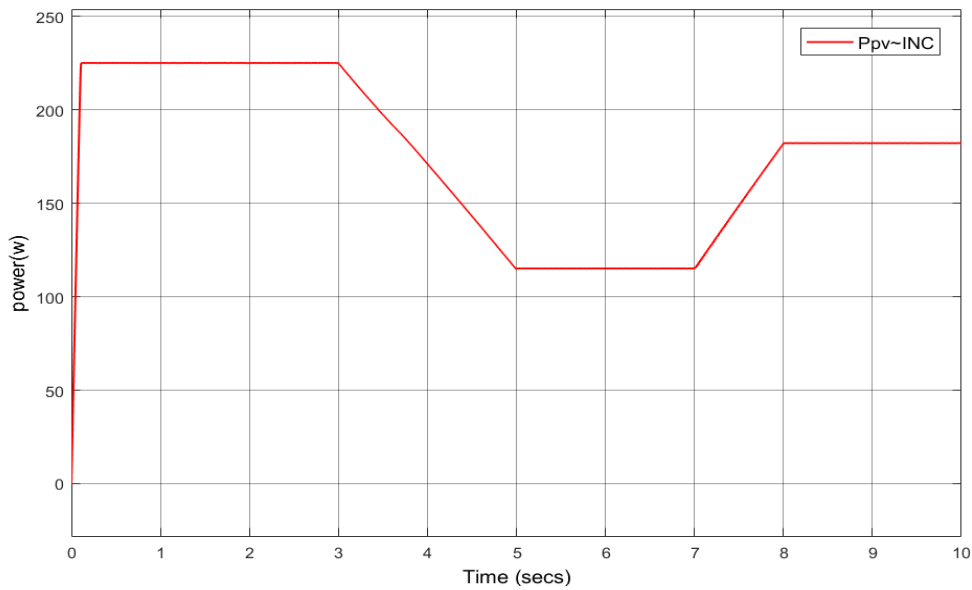


Figure III-27: Variation on Ppv under changing irradiance conditions.

➤ Temperature:

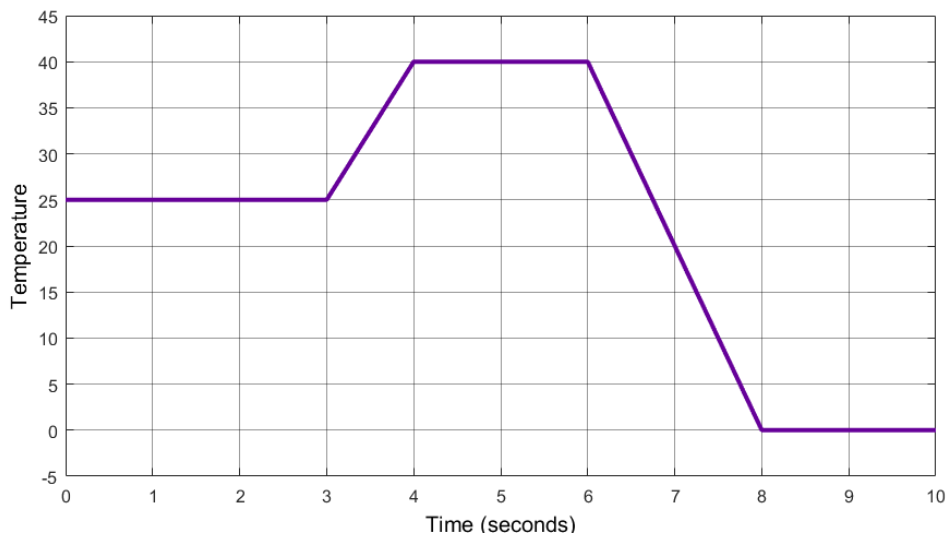


Figure III-28: Variation of temperature with time.

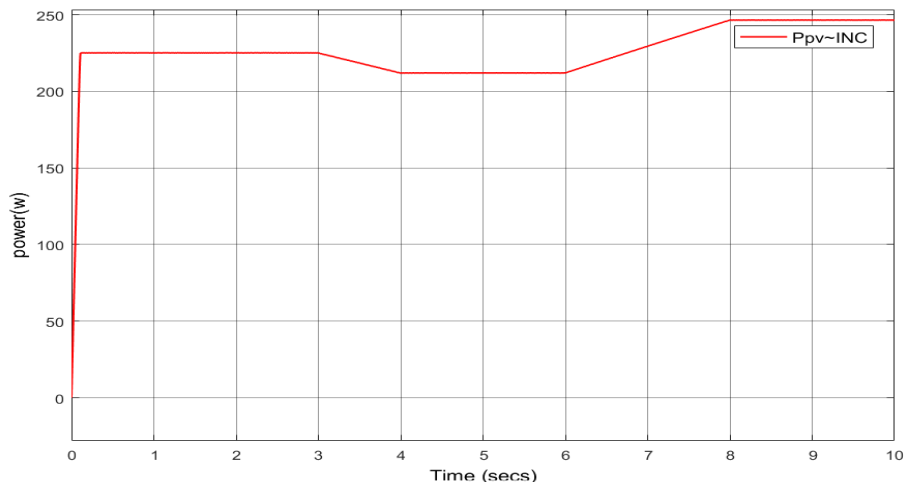


Figure III-29: Variation on Ppv under changing temperature conditions.

III.2.6 Particle swam optimization method

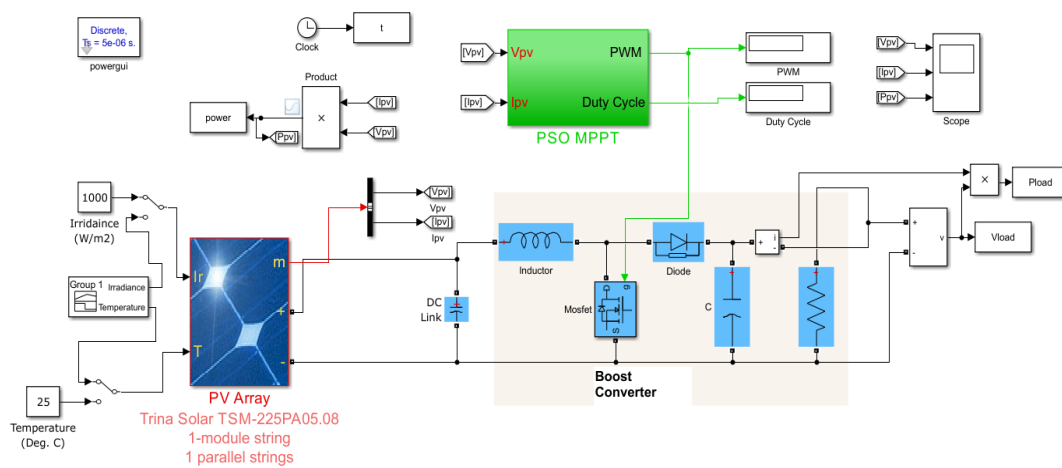


Figure III-30: Simulink diagram of a PV system using the PSO method.

- PSO Parameters are as follows:

Parameters	
PWM Switching frequency (Hz):	50000
Number of particles (3-8)	4
Inertia Weightage (w)	0.2
Acceleration Coefficient (c1)	1.2
Acceleration Coefficient (c2)	2

Figure III-31: PSO parameters.

- The following graphs are from the simulations:

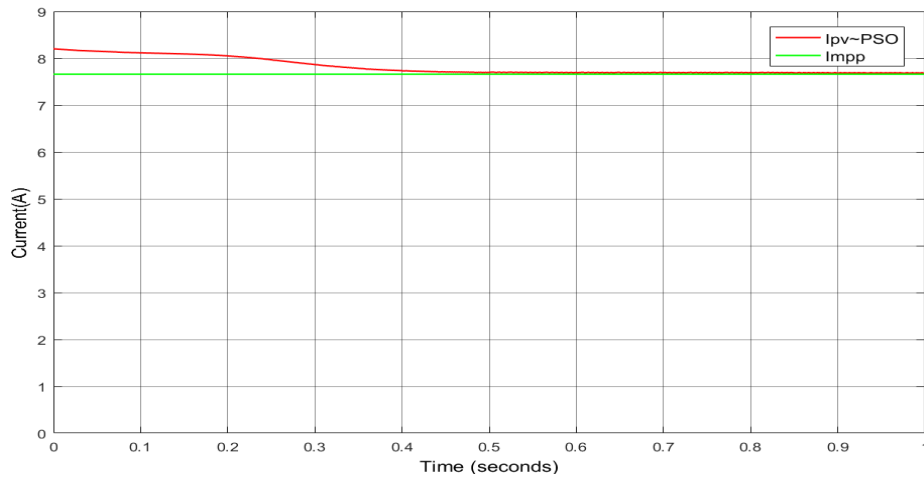


Figure III-32: PV current using PSO.

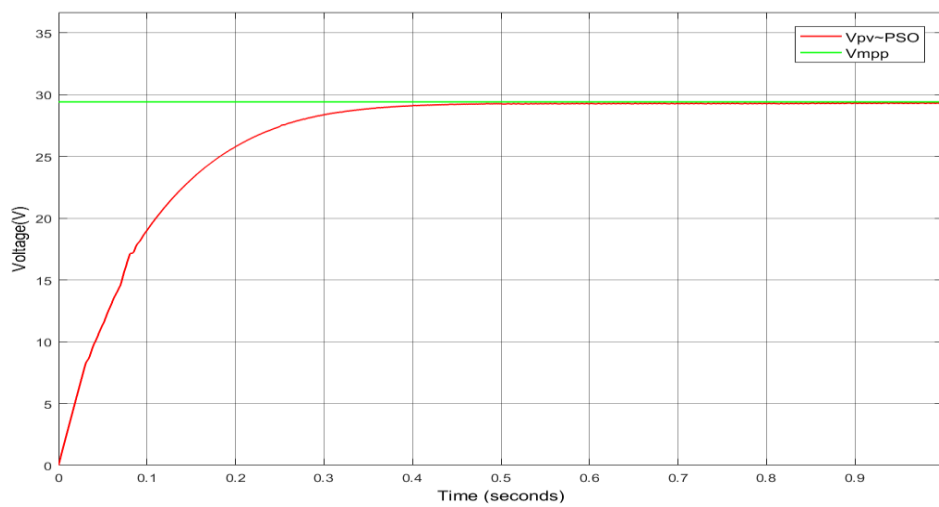


Figure III-33: PV voltage using PSO.

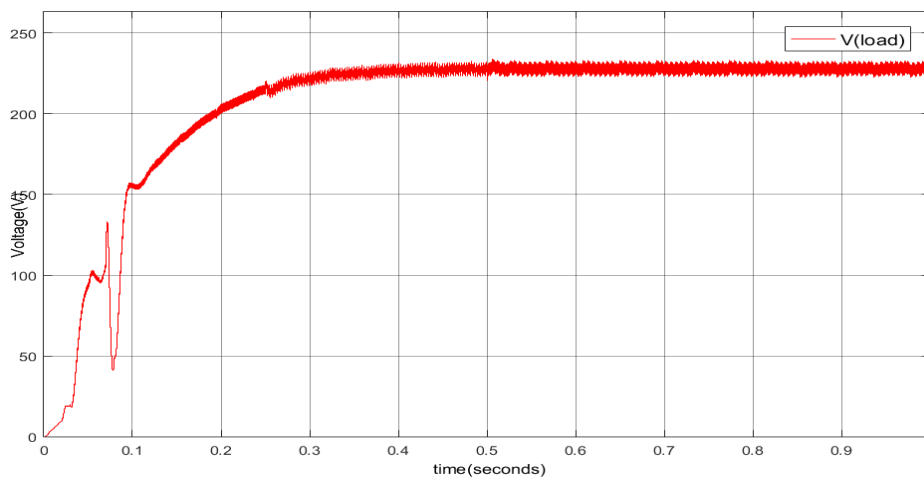


Figure III-34: Load voltage (across resistor) using PSO.

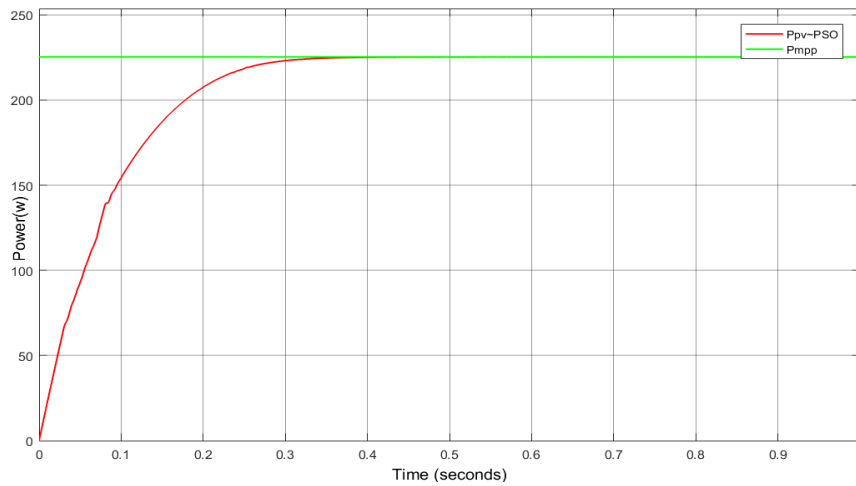


Figure III-35: PV power using PSO.

The PV current graph shows that the current decreases from an initial value which corresponds to the short-circuit current $I_{sc}=8.2$ A to oscillate around a value corresponding to the maximum power point current $I_{mpp}=7.66$ A.

The PV voltage shows that the evolution of the voltage has the same behavior as the steady state power, it oscillates around a value corresponding to the voltage of the maximum power point $V_{mpp}=29.4$ V.

The load voltage graph shows that the boost converter is functioning properly as the output voltage has been boosted and oscillates around a maximum value of around 225V. PV power graph shows that the value of power oscillates around the value corresponding to the power at mpp of the pv module $P_{mpp}=225.2$ W.

Secondly we are also obliged to study the effect of meteorological conditions on the tracking of maximum power points (**temperature and irradiance**)

➤ **Irradiance:**

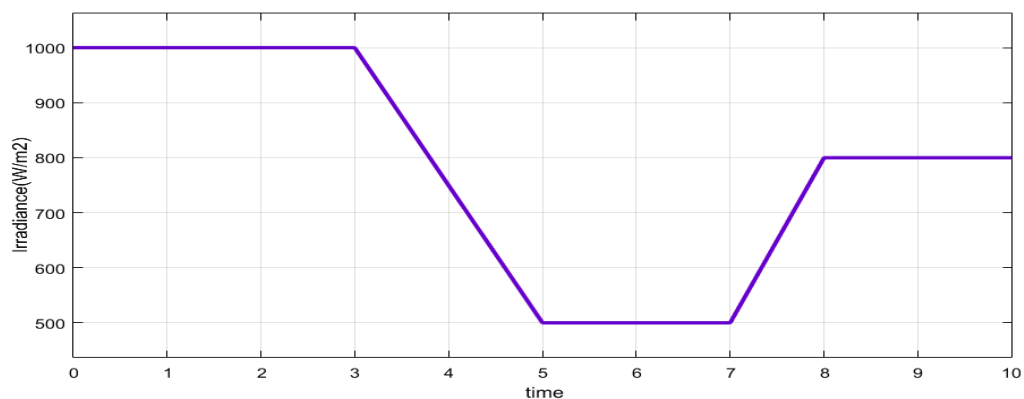


Figure III-36: Variation of irradiance with time.

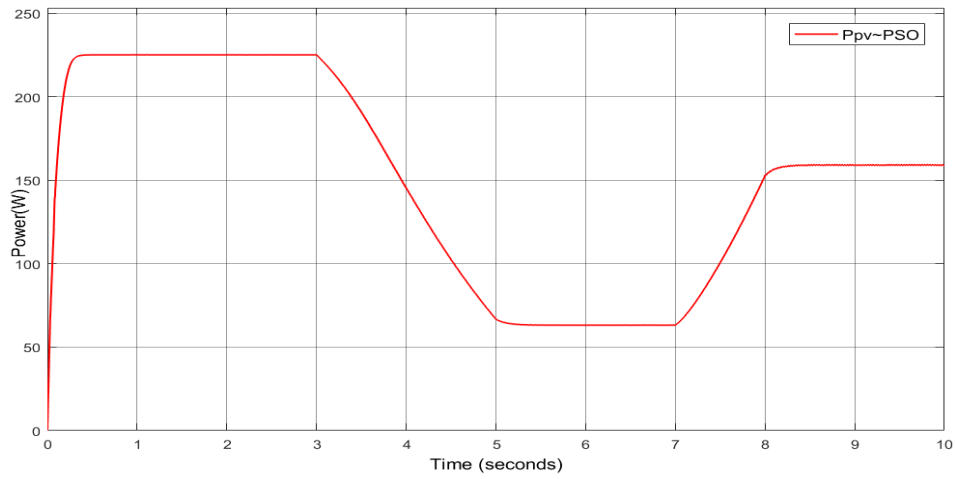


Figure III-37: Variation on Ppv under changing irradiance conditions.

➤ **Temperature:**

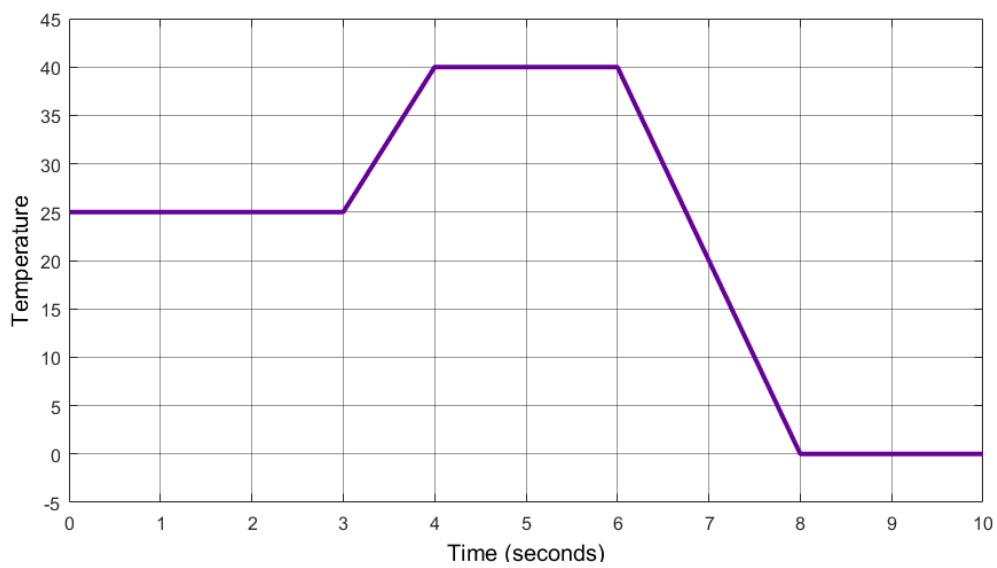


Figure III-38: Variation of temperature with time.

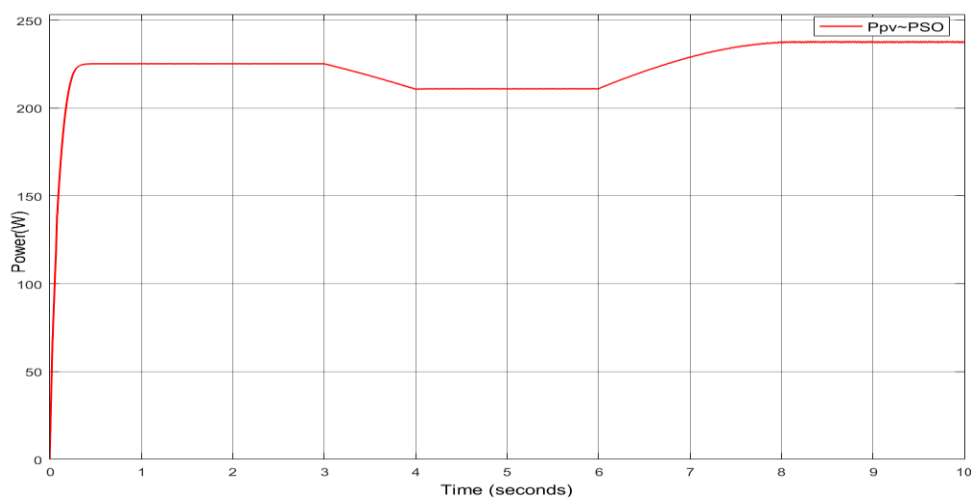


Figure III-39: Variation on Ppv under changing temperature conditions.

III.3 Comparison between the 3 MPPT methods (P&O, INC, PSO)

III.3.1 Response and tracking speed

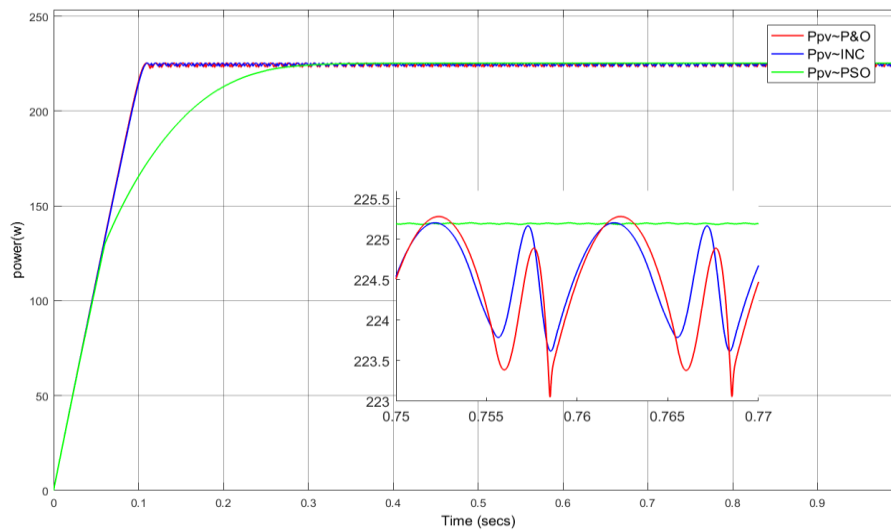


Figure III-40: Comparing PV power of P&O, INC, PSO.

As shown on the (**figure III-40**)

P&O and INC algorithms exhibit fast response and tracking speed, P&O algorithms have a relatively straightforward implementation, enabling rapid updates of the operating point. As for INC, the conductance (I/V) and its rate of change (dI/dV) are used to calculate the MPP. INC algorithms can swiftly update the operating point to monitor changes in environmental circumstances and maintain stability close to the MPP by comparing these factors. The quick modification based on conductance makes it possible to track the MPP quickly and effectively.

Comparing PSO algorithms to P&O and IC algorithms, tracking speed might be reasonable. PSO algorithms use swarm intelligence and optimization approaches to iteratively converge to the MPP. PSO methods can nevertheless deliver effective tracking in a reasonable amount of time, although possibly requiring more processing resources and repetitions to find the optimal operating point. Swarm size, convergence requirements, and the complexity of the optimization procedure are a few examples of variables that may have an impact on the tracking speed of PSO algorithms.

III.3.2 Accuracy and oscillations at MPP

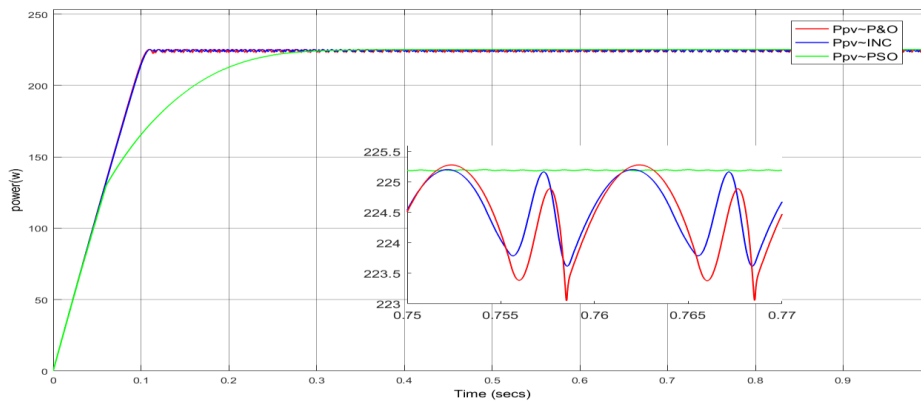


Figure III-41: Comparing oscillations of Ppv at MPP.

The graph of Ppv above shows that the PSO Technique is capable of tracking the MPP with high accuracy, particularly in steady meteorological conditions. It investigates the problem space and moves closer to the ideal operating point by using swarm intelligence and optimization approaches. PSO has less oscillations around the mpp as compared to P&O and IC.

Comparing oscillations output load voltage (Vload) after boost converter:

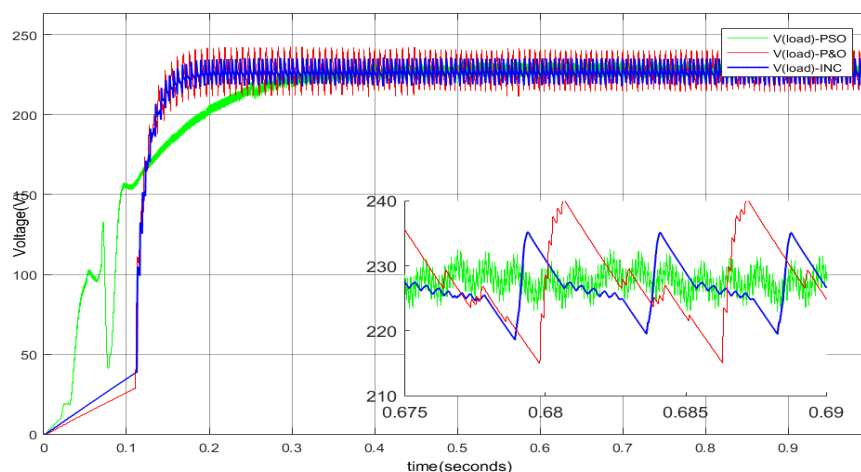


Figure III-42: Comparing oscillations of Vload at MPP.

Overall PSO exhibits the lowest level of ripple voltage at the load and oscillates the closest to the maximum power of our PV module of **225.204W**.

III.3.3 Settling time

When contrasting the P&O, IC and PSO approaches for Maximum Power Point Tracking, the settling time is a crucial factor to take into account. It refers to the amount of time an MPPT algorithm needs to settle and attain steady-state functioning.

By performing MATLAB command,

Stepinfo (power.Data, power.Time).

P&O	IC	PSO
0.1048	0.103	0.2555

Table III-2: Settling time.

Several major observations may be made when comparing the settling time of these MPPT systems. P&O, being a basic and frequently used MPPT approach, has a comparatively fast settling time. As for IC, with its incremental conductance approach, offers improved tracking accuracy and faster settling times compared to P&O. By continuously monitoring changes in conductance, this method quickly adapts to varying environmental conditions, leading to reduced settling time and enhanced stability.

PSO's optimization skills enable it to explore the search space effectively and converge on the global MPP. However, PSO's computational complexity may result in longer settling times as compared to P&O and IC.

III.3.4 Stability under changing conditions

➤ **Under rapidly changing irradiance:**

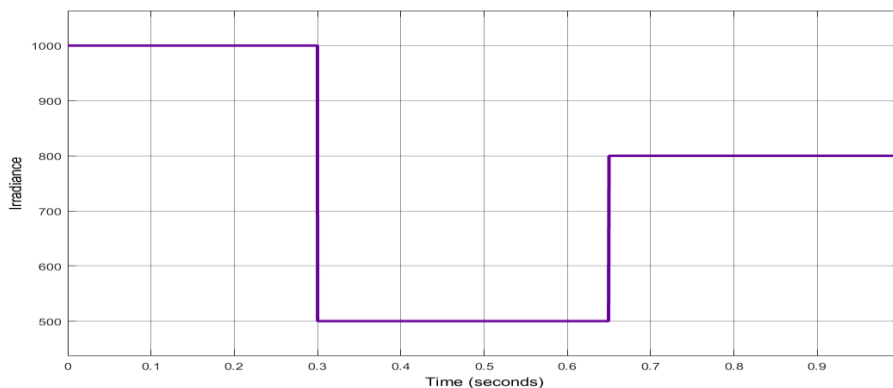


Figure III-43: Varying irradiance.

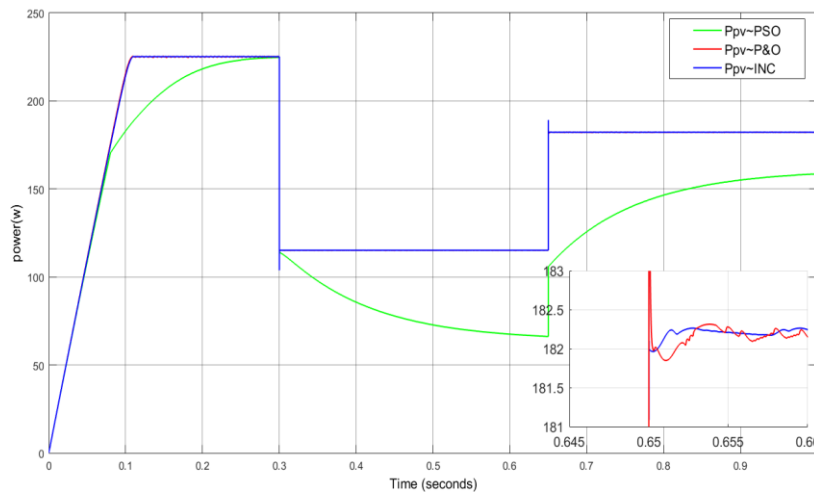


Figure III-44: PV power under rapidly varying irradiance.

In short, under rapidly changing weather conditions, the Incremental Conductance and Perturb and Observe MPPT algorithms generally exhibit better stability, response and speed compared to Particle Swarm Optimization algorithm.

PSO algorithm can face challenges in rapidly changing conditions due to several reasons:

- PSO algorithms need a number of iterations to reach the best operating point. It can be challenging for the particles to converge quickly when the environment is rapidly changing because this can cause considerable fluctuations in the power-output landscape. As a result, PSO algorithms' ability to efficiently track the maximum power point (MPP) may suffer from an increase in convergence time.
- PSO algorithms have various parameters that need to be tuned, such as inertia weight, acceleration coefficients, and swarm size. These variables affect how the algorithm searches and how quickly it converges. To ensure optimal performance under rapidly changing conditions, these parameters may need to be changed often. The algorithm may struggle to adapt to the changing circumstances and reach rapid convergence if the parameters are not set properly.

➤ **Under slowly changing irradiance:**

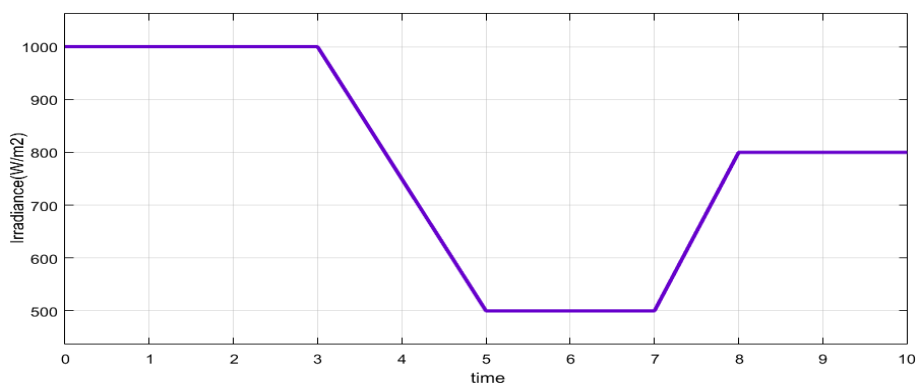


Figure III-45: Slowly varying irradiance.

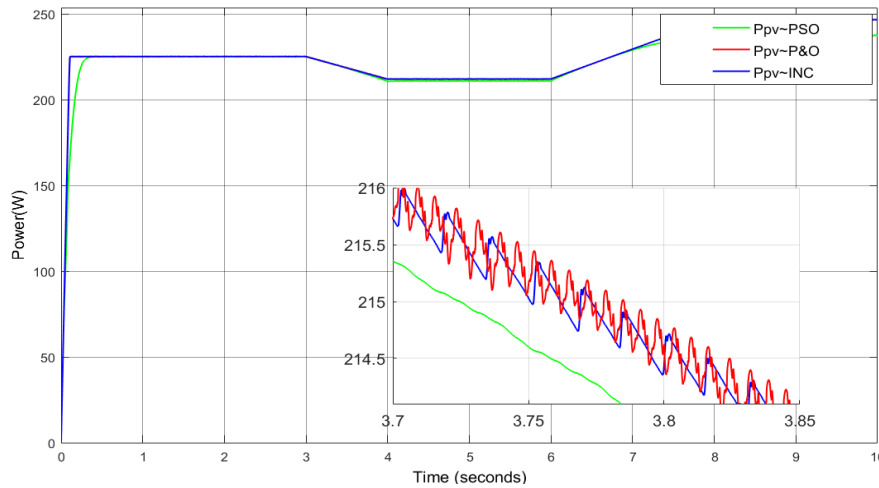


Figure III-46: PV power under slowly varying irradiance.

PSO tends to perform better under slowly changing condition.

III.3.5 Table of comparisons

This table compares MPPT algorithm techniques (P&O, IC, PSO) in terms of settling time, stability, oscillations, accuracy, tracking speed, and complexity. It helps in selecting the suitable method for a specific solar system.

Properties	P&O	IC	PSO
Settling time	0.1048	0.103	0.2555
Stability	Better	Best	Average
Oscillations at MPP	Average(depends on step size)	Average(depends on step size)	Very low
Accuracy	Good accuracy on normal conditions	Good accuracy(an improvement of P&O)	Very high accuracy
Tracking speed	Fast tracking	Fast tracking	Reasonable tracking speed
Complexity	Simple and easy to implement	More complex than P&O	Most complex intelligent algorithm

Table III-3: Summary of comparisons between P&O, IC and PSO.

III.4 Conclusion

Firstly, it was observed that all three MPPT techniques are effective in tracking the maximum power point of a PV system. Each technique demonstrated reasonable adaptation to changing environmental conditions and maintained efficient power extraction.

Regarding tracking efficiency, the P&O technique exhibited a simple nature, making it easy to implement and widely used in various applications. However, it suffered from a concerning amount of oscillations around MPP.

The IC technique, on the other hand, demonstrated improved tracking accuracy compared to P&O. It utilized the incremental change in conductance to determine the MPP, resulting in reduced oscillations and a faster response to varying environmental conditions. This technique proved to be more reliable and stable, showing superior performance over P&O in scenarios with dynamic irradiance levels.

Lastly, the PSO technique, based on swarm intelligence, exhibited excellent tracking accuracy and convergence to the MPP. It also showed little to none oscillations as it reached MPP. Its optimization capabilities allowed it to explore the search space efficiently and find the global maximum power point. However, the computational complexity and tuning of PSO parameters were found to be more demanding compared to P&O and IC.

In conclusion, each MPPT technique has its own strengths and weaknesses. The choice of technique depends on the specific application requirements, environmental conditions, and trade-offs between simplicity, efficiency, and accuracy. While P&O is commonly used due to its simplicity, IC offers improved accuracy, speed and stability. PSO provides the highest level of optimization with very high level of accurate tracking but requires more computational resources and tuning of parameters.

General conclusion

General conclusion

The work presented in this Masters dissertation focused mainly on comparing power maximization in PV systems while implementing the use of MPPT algorithms. The MPPT algorithms make it possible to control a DC-DC converter using PWM signals, therefore ensuring that the load is continuously supplied with maximum power in varying meteorological conditions. This work can simply be taken as a comparison between P&O, IC and PSO power maximization techniques with emphasis being on power extraction efficiency, response speed, and tracking accuracy.

To achieve these objectives, after presenting the basics on PV systems, we relied on the MATLAB/SIMULINK tool to create a virtual PV system. The PV module implemented produced a power of 250W under testing conditions with a temperature of 25°C and an irradiance level of 1000 W/m².

Next, we focused on the three MPPT techniques. We started by tackling the theoretical aspect of these algorithms and understood how they function to improve the power output of PV systems. The following step was to do the simulations to determine a proper step size to implement in P&O and IC. A step size of 0.001 proved to be the best as it showed fewer oscillations around MPP. Further simulations were also done using all the MPPT methods under varying temperature and irradiance levels.

Through an in-depth literature review and simulation-based analysis, several important findings were obtained. Firstly, P&O and IC algorithms demonstrated fast response times and relatively accurate tracking under steady-state conditions. However, they exhibited a few concerning oscillations around MPP as compared to a smoother PSO which showed very little oscillations. PSO algorithm also showcased slower convergence and response times, but provided a very high level of tracking accuracy and stability.

We can therefore very much conclude that:

- By using a DC-DC converter, we get an output voltage far superior than that produced by the PV module, therefore, it is ideally essential in implementing PV systems.
- The performance of PV system is vastly influenced by Irradiance and Temperature levels.
- MPPT techniques improve the efficiency of PV systems.
- When selecting a technique for a specific application, it is critical to consider the trade-offs between efficiency, response time, tracking accuracy, and complexity.

Prospects and future work:

This work can certainly be improved in the future with emphasis being on:

- Combining the algorithms into hybrids like PO-PSO and IC-PSO.
- Using modern PSO based methods like Chaotic Particle Swarm Optimization and Fuzzy Particle Swarm Optimization.
- Carrying out the investigation in a real life environment.

Bibliography

Introduction

- [1] S. Cherifi and M. Haddad, "L'énergie solaire : un moteur du développement durable en Algérie ", Les Cahiers du Cread, 35(03), pp 125, 2020.
- [2] I. K., Bayal, Ö, Kurtuluş, G., Baş, Y., Gültekin, A., Öztürk and Özbay, " Examination of the temperature related structural defects of InGaN/GaN solar cells", Superlattices and Microstructures, 86, pp 379-389, 2015.

Chapter I

- [3] I.F. Bouguenna, "Modélisation et Optimisation d'une Cellule Solaire Tandem a-Si:H/a-SiGe ", Masters Dissertation, University of Oran Mohamed Boudiaf , 2009.
- [4] S. Michael, A. D. Bates and M. S. Green, "Silvaco ATLAS as a solar cell modeling tool," Conference Record of the Thirty-first IEEE Photovoltaic Specialists Conference, Lake Buena Vista, FL, USA, 2005, pp. 719-721, doi: 10.1109/PVSC.2005.1488232.
- [5] C. Richter, D. Lincot and C.A. Gueymard, "Solar Energy", Springer New York, 2012.
- [6] C. Honsberg and S. Bowden, "Photovoltaics: Devices, Systems and Applications", <http://pvcadrom.pveducation.org/index.html>, 2009.
- [7] M.A.Green, "Solar cells: Operating principles, technology, and system applications", Prentice-Hall, UK, 1982.
- [8] ASTM, "Standard Table for Reference solar irradiances: Direct, Normal and Hemispherical on 37 degree tilted surface", Conshohocken, PA, 2003.
- [9] NREL, "Reference Air Mass 1.5 Spectra", NREL, <https://www.nrel.gov/grid/solar-resource/spectra-am1.5.html>, (accessed May 18 2023).
- [10] A. MEDJHED, "Extraction des paramètres des cellules solaires en utilisant le modèle à deux exponentielles ", Masters Dissertation, University of Setif, 2011.
- [11] ElectricalVoice, "Material Classification based on Energy Band Diagram", ElectricalVoice, <https://electricalvoice.com/material-classification-based-energy-band-diagram/>, (accessed May 19, 2023).
- [12] A. Chovet and P. Masson, "Physique des semi-conducteurs ", 1st Year course, École Polytechnique- Université De Marseille, 2004 -2005
- [13] ElectroDuino, "PN Junction Diode – Formation, Symbol, Biasing, V-I Characteristics, Application", Electroduino, <https://www.electroduino.com/pn-junction-diode-formation-symbol-biasing-v-i-characteristics-application/> , (accessed May 19, 2023).

- [14] H. Mathieu H. Fanet, “ Physique des semiconducteurs et des composants électroniques ”,6th Edition, Dunod, 2009
- [15] S. M. Sze, “Semiconductor Devices”, 2nd Edition, Wiley India, pp. 77-133, 2008,
- [16] H. Mathieu, "Physique des semi-conducteurs et des composants électroniques", 2nd Edition, Masson ,1990.
- [17] M. Madani, “Réalisation Des Couches Antireflets Dans Les Cellules Solaires a Couches Minces ”, Masters Dissertation, University of Tlemcen, 2006
- [18] S.Quoizola, “ Epitaxie en phase valeur de silicium sur silicium me soporeux pour report sur Substrats économiques et application photovoltaïque bas cout ”, Doctoral Thesis, Ecole Doctorale : Electronique, Electrotechnique et Automatisme, L’institut National des Sciences appliquées de Lyon ,2003
- [19] S. M. Sze, K. N. Kwok, “ Physics of Semiconductor Devices”, 3rd edition, Wiley Interscience, New Jersey, pp. 77-133, 2006, <https://doi.org/10.1002/9780470068328.ch2>
- [20] Khudayer, Iman. (2017). Study of Physical and Optoelectronic Properties of CuInSe2/Si Heterojunction Solar Cells. Energy Procedia. 119. 507-517. 10.1016/j.egypro.2017.07.062.
- [21] S. Alem-Boudjemline, “ Réalisation et caractérisation de de cellule photovoltaïque plastiques ” ,Doctoral Thesis, University of Angers, 2004.
- [22] J. Royer, T. Djiako, E. Schiller, B .Sada Sy, “Le pompage photovoltaïque» manuel de cours à l’intention des ingénieurs et des techniciens ”, édition Multi Mondes IEPF/Université d’Ottawa/EIER/CREPA,1998,https://www.pseau.org/outils/ouvrages/iepf_pompage_photovoltaique.pdf
- [23] D. Santosh, “Solar Photovoltaic Panel System”, Electronics and You, <https://www.electronicandyou.com/solar-photovoltaic-panel-system.html> , (accessed May 21, 2023).
- [24]A. Bensalem and M. Benkaihou, “Development of a multi-output I-V tracer for the characterization of photovoltaic modules”, Masters Dissertation, University of M’sila, 2022
- [25] S. K. Sharma and K. Ali, “SOLAR CELLS: materials to device technology”, Springer, 2020, <https://link.springer.com/book/10.1007/978-3-030-36354-3>
- [26] L.A Lamont, “History of Photovoltaics, in Comprehensive Renewable Energy”, Elsevier, vol 1, pp 31 – 45, 2012, doi: 10.1016/B978-0-08-087872-0.00102-5.
- [27] M. Bencherif, “Modélisation de système énergétique photovoltaïque et éoliens intégration dans système hybride base tension ”, Doctoral Thesis, University of Tlemcen, 2013
- [28] Circuit Globe, “Photovoltaic or Solar Cell”, Circuit Globe, <https://circuitglobe.com/photovoltaicorsolarcell.html#:~:text=Definition%3A%20The%20Pho>

[tovoltaic%20cell%20is,of%20their%20voltage%20producing%20capability](#).(accessed May 30, 2023).

- [28] A. Mahfoud, “Modélisation des cellules solaires tandem à couches minces et à haut rendement”, Doctoral Thesis, Université de Setif-1, 2015
- [29] S. Alem-Boudjemline. “Réalisation et caractérisation de de cellule photovoltaïque plastiques”, Doctoral Thesis, Université d’Angers, 2004
- [30] F. Menacer, “Simulation des cellules solaires en InGaN en utilisant Atlas Silvaco”, Masters Dissertation, Université Mohamed Khider – Biskra, 2016
- [31] T. Mambrini, “Caractérisation de panneaux solaires photovoltaïques en conditions réelles d’implantation et en fonction des différentes technologies”, Doctoral Thesis, University of South Paris- Paris XI, 2014
- [32] F. A. Lindholm, J.G. Fossum, and E.L. Burgess, “Application of the superposition principle to solar-cell analysis”, IEEE Transactions on Electron Devices, vol. 26, pp. 165–171, 1979
- [33] F. Ghaleb, K. Bendjbar and S. Haouari, “Étude et Simulation des paramètres électriques d’une cellule solaire photovoltaïque à base de Silicium”, Masters dissertation, University of Tizi-Ouzou, 2015.
- [34] M.R. Belmeliani and W. Youcef, " Modélisation d’un système photovoltaïque relié au réseau : Contrôle des puissances active et réactive”, Masters dissertation, University of Mascara Mustapha Stambouli, 2018.
- [35]K. Sardashti, “A comprehensive review of the efficiency enhancement techniques in CdTe and OPV solar cells”, Renewable and Sustainable Energy Reviews, 2019

Chapter II

- [36] Mepits, “MPPT or PWM??? which is better?,” Mepits, <https://www.mepits.com/tutorial/579/electrical/mppt-or-pwm-which-is-better> (accessed May 29, 2023).
- [37] G. Pillonnet, M. Hmada, and P. Mercier, «Normalized Benchmarking of Hybrid Switched-Capacitor DC-DC Converters,” Department of Electrical & Computer Engineering, University of California San Diego, May 2023
- [38]J.K. Chauhan, P. Chauhan, T. Maniar and A. Joshi, “Comparison of MPPT algorithms for DC-DC converters based photovoltaic systems”, International Conference on Energy Efficient Technologies for Sustainability, pp. 476-481, 2013

- [39] A. E. Kayode and M. Franchesca, "Comparative study of Mppt controls applied to a photovoltaic system connected to the Electrical network", Masters Dissertation, Faculty of Technology, University of Tlemcen, pp. 70-74, 2022
- [40] M. Bedrane, "Étude comparative entre quelques méthodes de poursuite du point de puissance maximale dans les systèmes photovoltaïques," Masters dissertation, University of Bejaia, 2013
- [41] R. Jiang, H. Michaels, N. Vlachopoulos, and M. Freitag, "Beyond the Limitations of Dye-Sensitized Solar Cells", *Dye-Sensitized Solar Cells: Mathematical Modelling, and Materials Design and Optimization*, pp. 285–323, Jan. 2019, doi:10.1016/B978-0-12-814541-8.00008-2.
- [42] J. Ahmed, Z. Salam, "An improved perturb and observe (P&O) maximum power point tracking (MPPT) algorithm for higher efficiency," *Applied Energy*, 150, pp. 97–108, 2015. <https://doi.org/10.1016/J.APENERGY.2015.04.006>
- [43] M. Kamran., M. Mudassar, M.U Asghar, M. Bilal and R. Asghar, "Implementation of improved Perturb & Observe MPPT technique with confined search space for standalone photovoltaic system," *Journal of King Saud University - Engineering Sciences*, 32(7), pp. 432–441, 2020, <https://doi.org/10.1016/J.JKSUES.2018.04.006>
- [44] A. Ali, K. Almutairi and M. Zahir, "Investigation of MPPT Techniques under Uniform and Non-Uniform Solar Irradiation Condition-A Retrospection', *IEEE Access*, vol. 8, pp. 127368–127392, 2020, doi: 10.1109/ACCESS.2020.3007710
- [45] H. Bounechba, A. Bouzid, K. Nabti, and H. Benalla, "Comparison of perturb & observe and fuzzy logic in maximum power point tracker for PV systems", *Energy Procedia*, vol. 50, pp. 677–684, 2014, doi: 10.1016/J.EGYPRO.2014.06.083.
- [46]— [39] pp 85-86
- [47] P. S. Gavhane, S. Krishnamurthy, R. Dixit, J. P. Ram, and N. Rajasekar, "EL-PSO based MPPT for Solar PV under Partial Shaded Condition", *Energy Procedia*, vol. 117, pp. 1047–1053, 2017, doi: 10.1016/J.EGYPRO.2017.05.227
- [48] R. I. Putri, S. Wiyanto, I. N. Syamsiana, M. Junus, M. Rifa'I, and E. S. Putra, "Maximum power point tracking based on particle swarm optimization for photovoltaic system on greenhouse application", *J Phys Conf Ser*, vol. 1402, no. 3, p. 033104, Dec. 2019, doi:10.1088/1742-6596/1402/3/033104.
- [49] O. Belghith, L. Sbita and F. Bettaher, "MPPT Design Using PSO Technique for Photovoltaic System Control Comparing to Fuzzy Logic and P&O Controllers ", *Energy and Power Engineering*, 8, pp. 349-366, 2016 doi: 10.4236/epe.2016.811031.
- [50] M. H. Ibrahim, S. P. Ang, M. N. Dani, M. I. Rahman, R. Petra, and S. M. Sulthan, "Optimizing Step-Size of Perturb and Observe and Incremental Conductance MPPT

Techniques Using PSO for Grid-Tied PV System”, IEEE Access, 2023, doi:10.1109/ACCESS.2023.3242979.

[51] B. Masood, M.S. Saddique and R.M. Asif “Maximum power point tracking using hybrid perturb & observe and incremental conductance techniques”, 4th ICE2T, 2014, doi: 10.1109/ICE2T.2014.7006277

[52] I.W. Christopher and R. Ramesh, “Comparative Study of P&O and InC MPPT Algorithms”, American Journal of Engineering Research, Volume-02, Issue-12, pp. 402-408, 2013

[53] L. Shang, H. Guo and W. Zhu, “an improved MPPT control strategy based on incremental conductance algorithm, ” Prot Control Mod Power Syst 5, 14, 2020, <https://doi.org/10.1186/s41601-020-00161->

Chapter III

[54] P. Kapadeeya and R.P Sukhadia, “Modelling and simulation of boost converter for solar pv system”, International Journal For Technological Research In Engineering, 2016, <https://ijtre.com/images/scripts/2016030741.pdf>

Abstract

This dissertation presents a comprehensive comparative study of three power maximization techniques, namely P&O, IC and PSO in PV systems. The study's objective is to evaluate and contrast how well these techniques perform in terms of power extraction effectiveness, response time, and tracking precision. The research begins with an in-depth literature review to establish the theoretical background and understanding of the three power maximization techniques, emphasis being on how they control boost converters using a PWM signal. The P&O and IC algorithms, which are commonly used in PV systems, are investigated and analyzed, highlighting their operational principles, advantages, and limitations. The PSO algorithm, a population-based optimization method, is introduced as a potential alternative for power maximization in PV systems. A comprehensive simulation model is developed using MATLAB/SIMULINK tool to simulate and evaluate the performance of the three techniques. The model considers various factors, including the characteristics of the PV modules, environmental conditions, and system parameters. The simulation results are analyzed to assess the power extraction efficiency, response speed, and tracking accuracy of each technique under various conditions. It is observed that P&O and IC algorithms provide fast response times and relatively accurate tracking in steady conditions. However, they can suffer from drastic oscillations meaning significant power losses in tracking MPP. On the other hand, PSO exhibits slower convergence and response times but offers improved tracking accuracy and stability, with very little to no oscillations around MPP. The dissertation also explores the impact of algorithm parameters such as step size on P&O and IC. The optimization of parameters for P&O, IC, and PSO algorithms is investigated to enhance their performance and achieve optimal power extraction efficiency. Overall, this dissertation contributes to the understanding of power maximization techniques in PV systems by conducting a comprehensive comparative study of P&O, IC, and PSO algorithms. The findings provide valuable insights for system designers and researchers to choose the most appropriate technique based on the specific requirements of the PV system, environmental conditions, and desired performance criteria.

Keywords: PV SYSTEMS, MPPT, P&O, IC, PSO, MATLAB/SIMULINK, BOOST CONVERTER

Résumé

Cette thèse présente une étude comparative complète de trois techniques de maximisation de puissance, à savoir P&O, IC et PSO, dans les systèmes photovoltaïques. L'objectif de l'étude est d'évaluer et de comparer l'efficacité de ces techniques en termes d'extraction de puissance, de temps de réponse et de précision de suivi. La recherche commence par une revue approfondie de la littérature afin d'établir les bases théoriques et la compréhension des trois techniques de maximisation de puissance, en mettant l'accent sur la manière dont elles contrôlent les convertisseurs élévateurs à l'aide d'un signal PWM. Les algorithmes P&O et IC, couramment utilisés dans les systèmes photovoltaïques, sont étudiés et analysés, en mettant en évidence leurs principes de fonctionnement, leurs avantages et leurs limites. L'algorithme PSO, une méthode d'optimisation basée sur la population, est présenté comme une alternative potentielle pour la maximisation de puissance dans les systèmes photovoltaïques. Un modèle de simulation complet est développé à l'aide de l'outil MATLAB/SIMULINK pour simuler et évaluer les performances des trois techniques. Le modèle prend en compte différents facteurs, notamment les caractéristiques des modules photovoltaïques, les conditions environnementales et les paramètres du système. Les résultats de la simulation sont analysés pour évaluer l'efficacité de l'extraction de puissance, la vitesse de réponse et la précision de suivi de chaque technique dans différentes conditions. On observe que les algorithmes P&O et IC offrent des temps de réponse rapides et un suivi relativement précis dans des conditions stables. Cependant, ils peuvent souffrir d'oscillations drastiques, ce qui entraîne des pertes de puissance significatives lors du suivi du point de puissance maximale. En revanche, le PSO présente une convergence et des temps de réponse plus lents, mais offre une meilleure précision de suivi et une stabilité accrue, avec très peu voire pas d'oscillations autour du point de puissance maximale. La thèse explore également l'impact des paramètres de l'algorithme tels que la taille de pas sur P&O et IC. L'optimisation des paramètres pour les algorithmes P&O, IC et PSO est étudiée afin d'améliorer leurs performances et d'atteindre une efficacité d'extraction de puissance optimale. Dans l'ensemble, cette thèse contribue à la compréhension des techniques de maximisation de puissance dans les systèmes photovoltaïques en réalisant une étude comparative complète des algorithmes P&O, IC et PSO. Les résultats fournissent des informations précieuses aux concepteurs de systèmes et aux chercheurs pour choisir la technique la plus appropriée en fonction des exigences spécifiques du système photovoltaïque, des conditions environnementales et des critères de performance souhaités.

Mots-clés: SYSTÈMES PHOTOVOLTAÏQUES, MPPT, P&O, IC, PSO, MATLAB/SIMULINK, CONVERTISSEUR ÉLÉVATEUR.